



University of Natural Resources
and Life Sciences, Vienna



Delft University of Technology

Master thesis

Snow cover in the Greater Alpine Region (2000 – 2017): regional patterns, controls and change

Hosted at the ¹Institute of Water Management, Hydrology and Hydraulic Engineering,
University of Natural Resources and Life Sciences (BOKU), Austria

With a guest stay at the ²Department of Water Management,
Delft University of Technology (TU Delft), Netherlands

Supervised by:

¹Karsten Schulz, Univ.Prof. Dipl.Geoökol. Dr.rer.nat.

²Markus Hrachowitz, Priv.Do. Dipl.-Ing. Dr.nat.techn.

Authored by:

Stefan Fugger, BSc

Submitted: July 2018

Acknowledgements

I would like to thank Karsten Schulz, who initially drew my attention to hydrological issues during his lectures, for valuable inputs and reliable supervising at decisive stages of my thesis. My appreciations also go to Markus Hrachowitz, who hosted my prolific guest stay at TU Delft, for offering thorough guidance throughout the whole process of my research and sharing his enthusiasm for the field of study.

Special thanks go to Christian Bouman for productive teamwork and numerous brainstorming sessions. Equally helpful was Juraj Parajka, who shared professional expertise and his collection of data on snow depth for Austria. Furthermore, I want to thank Susan Steele-Dunne for valuable remote-sensing-related ideas as well as Matthew Herrnegger for his interest and advice on various issues related to my research.

Declaration of academic honesty

I hereby declare that I am the sole author of this work. No assistance other than that which is permitted has been used. Ideas and quotes taken directly or indirectly from other sources are identified as such. This written work has not yet been submitted in any part.

Eidesstaatliche Erklärung

Hiermit versichere ich, die vorliegende Masterarbeit eigenständig und nach bestem Wissen und Gewissen verfasst zu haben. Es wurden keine weiteren, bis auf die von mir im Literaturverzeichnis angeführten Quellen verwendet, die in der vorliegenden Arbeit als solche gekennzeichnet sind. Sämtliche abgeleiteten Quellen wie Datensätze oder Illustrationen wurden als solche hervorgehoben.

Stefan Fugger

Abstract

Water retained in the snow packs and glaciers of mountainous regions is fundamentally important to the maintenance of downstream ecosystems, including societies. This study aims to assess and interpret changes in the dynamics of annual snow cover duration and regional patterns thereof over the 2000-2017 period. MODIS snow cover products were analysed using the Regional Snowline Elevation (RSLE) method, which was adapted and extended as a means for large-scale cloud cover reduction. To quantify the snow cover duration, the annual number of days with snow cover (D_{sc}) was derived at 100m steps from the resulting RSLE time series. An upward shift of the RSLE was identified for most parts of the GAR, which translates into partly significant reductions of annual snow cover duration by up to -35 days, (i.e. $\sim 2 \text{ d yr}^{-1}$) over the study period. The data suggest that intermediate and higher elevations (~ 1200 to 3400m), especially north of the main alpine ridge experienced most pronounced changes in D_{sc} , while south of the main alpine ridge and at lower elevations, the GAR shows only few significant changes. Estimates of D_{sc} , derived from MODIS snow cover data correspond well with D_{sc} derived from point-scale data from various ground station observations. The combined analysis of D_{sc} , winter temperature (wT) and annual cumulative solid precipitation (csP) allowed for an exploration into the varying roles of wT and csP in controlling D_{sc} , depending on geographical position and elevation. Further consideration of trends showed that changes in wT caused a reduction of D_{sc} , even at locations where csP increased.

Contents

- Acknowledgements 1
- Declaration of academic honesty 2
- Abstract 3
- 1. Introduction 5
- 2. Study Domain 8
- 3. Data & Methods 10
 - 3.1. Regional snow line elevation (RSLE) 11
 - 3.2. Influence of exposure to solar radiation 13
 - 3.3. Annual number of days snow covered (D_{sc}) 14
 - 3.4. Trend analysis 15
 - 3.5. Relating D_{sc} to temperature and precipitation 16
- 4. Results 18
 - 4.1. Regional snow line elevation (RSLE) 18
 - 4.2. Influence of exposure to solar radiation 18
 - 4.3. Annual number of days snow covered (D_{sc}) 18
 - 4.4. Trend analysis 19
 - 4.5. Relating D_{sc} to temperature and precipitation 19
- 5. Discussion 21
- 6. Conclusions 25
- Bibliography 26
- Appendix - Results 31

1. Introduction

Water retained in the snow packs and glaciers of mountainous regions is fundamentally important to the maintenance of downstream ecosystems, including societies. In the same regions, snowmelt affects the timing and magnitude of spring floods (Molini et al., 2011; Parajka et al., 2010), as well as hydropower generation (Madani and Lund, 2010). Snow cover (albedo back-scattering) is an important factor to the regional and global energy balance (Déry and Brown, 2007; Fernandes et al., 2009) and is furthermore a crucial economic factor concerning the recreational industry (e.g. Elsasser and Bürki, 2002; Steiger and Abegg, 2016).

However, climate change is expected to severely affect the mountain cryosphere (Beniston et al., 2018), including snow dynamics, potentially leading to changes in hydrological regimes (e.g. Barnett et al., 2005; Berghuijs et al., 2014; Hrachowitz et al., 2013; Jenicek et al., 2018), changes in the characteristics of extreme events (Laaha et al., 2016; Meißl et al., 2017) and putting considerable parts of the available water storage in snow at risk (Mankin et al., 2015). “How much (snow) can we save?” was asked by Marty et al. (2017a), who, as well as Verfaillie et al. (2018), predicted potential changes in snow depth under different climate change scenarios. Similarly, Marke et al. (2015) provided projections of D_{sc} for the Schladming region in the context of ski tourism.

Snow accumulation and melt are controlled by multiple interacting factors including the entire range of climate elements, large scale weather patterns, solar radiation, geographical location, topography, vegetation, artificial snow production and aerosols (-deposition). They are thus characterized by high spatio-temporal heterogeneity and remain challenging to describe with available observation methods. To hydrologists, the knowledge of past, present, and projected snow pack properties, especially the amount of water stored and released (snow water equivalent - SWE) is most relevant for applications like hydrological model calibration, runoff forecasting and prediction. Yet it is the one property that is most challenging to quantify and model (Mudryk et al., 2015; Räisänen, 2008). One of the few studies conducted for the Alps involving observed SWE (Marty et al. 2017b) showed, that spring-SWE has decreased at all investigated elevations and locations during the last six decades with higher, but less significant trends in lower regions.

Because of the low availability of SWE data, most snow climatological studies are dealing with metrics related to the extent of snow cover, e.g. snow line elevation, snow covered duration (SCD), snow covered area (SCA) or dates of onset and melt-out. These studies vary in scale from regional to hemispherical and roughly split into observation-based and model-based approaches. While the latter ones deal with reanalysis data derived from climate models (Durand et al., 2009; Formayer and Nadeem, 2012), observation-based studies can be further split into studies focusing on ground station measurements (e.g. Marty, 2008; Scherrer et al., 2013; Valt and Cianfarra, 2010) or on remote sensing products (Allchin and Déry, 2017; Immerzeel et al., 2009; Painter et al., 2009; Stehr and Aguayo, 2017). Time series of snow depth from ground stations are potentially rich in information at the point scale, yet often fail to be regionally representative due to effects like exposure, preferential deposition and snowdrift

(Lehning et al., 2008). Such measurement stations exist mostly in regions where snow data is of high economic and/or scientific relevance and at locations and elevations where daily monitoring is feasible throughout the snow season. For example, Klein et al. (2016) analysed a set of swiss snow depth stations between 1100 and 2500 m.a.s.l for the period 1970 to 2015 and found an average shortening of the snow season by 12 and 26 days in autumn and spring respectively.

Snow cover products from optical remote sensing can potentially offset some of the problems connected to point-scale data, however come with other major drawbacks: To this date, time series at a sufficient spatial and/or temporal resolution for consistent regional snow cover analysis are still short and the information content is limited to the snow cover extent. Furthermore, there is a lack of continuous time series due to cloud cover obscuration, e.g. 63% average cloud cover over Austria (Parajka and Blöschl, 2006). Yet, they can serve as a valuable data source for snow-climatological applications due to their potential inform about snow cover in spatial and temporal detail (Immerzeel et al., 2009). A variety of remote sensing products for snow cover mapping exist. But once a certain spatial and temporal resolution is desired, options shrink drastically. For example, data from the NOAA-AVHRR were used for continental-scale analysis, identifying SCD as the snow-related variable most sensitive to change (Brown and Mote, 2009) with significantly negative trends over western Eurasia (Hori et al., 2017). Yet, the low spatial resolution of that product (highest: 4km, for most recent imagery) does not allow for a more detailed analysis, particularly in mountain regions. With 16 days return period, LANDSAT imagery fails to provide sufficient temporal resolution to capture the snow cover dynamics during periods of snow accumulation and depletion. However, its spatial resolution (i.e. 30m) previously proved valuable for testing other snow cover products (Crawford, 2015; Gascoin et al., 2015; Rittger et al., 2013; Tang et al., 2013).

In contrast, the MODIS snow cover products (i.e. Terra MOD10A1 and Aqua MYD10A1, Hall et al., 2002), which come at a sub-daily temporal, and a 500m spatial resolution, provide a trade-off that allows enough detail for both, understanding spatial snow cover patterns as well as it's temporal dynamics. They are frequently applied for various types of climatological and hydrological studies (e.g. Andreadis and Lettenmaier, 2006; Dietz et al., 2012; Gascoin et al., 2015; Nijzink, 2018; Tomaszewska and Henebry, 2018). Accuracy assessments against ground station data in different regions found overall accuracy-levels for non-cloud-filtered imagery ranging from 93% (Hall and Riggs, 2007) to 95% (Parajka and Blöschl, 2006), with lowest values at forested sites (Parajka et al., 2012). A range of methods to deal with cloud-obscuration has been developed and applied, mostly keeping high accuracy levels, including the combination of Terra and Aqua snow maps, spatio-temporal filtering, use of snow depth data and snow-line filtering (Dietz et al., 2012; Dong and Menzel, 2016; Gafurov and Bárdossy, 2009; Parajka and Blöschl, 2008). Another efficient cloud filter, with an overall accuracy of 86%, was introduced with the Regional Snow Line Elevation (RSLE) method by Krajci et al., (2014) which potentially produces a “gap-free” time series of snow line elevation, that can be used directly for various further applications. Doing so, Krajčí et al. (2016) analysed snow line dynamics, snow covered area and snow depletion curves for 10 Slovak catchments for the

period 2001 to 2014. They did not find clear trends in mean annual snow-covered area, but a period of snow rich winters followed by a period of snow scarce winters.

While studies on snow cover distribution in space and time are abundant, links between snow cover and different climate elements gained less attention. Formayer and Nadeem (2012) explained large inter-alpine differences in mean snow line elevation with the temperature differences of arriving air masses, the origin of these air masses and orographic effects. They also found large decadal anomalies of mean snow line elevation for the GAR and related a 1°C temperature anomaly to a 150m difference in snowline elevation. Sospedra-Alfonso et al. (2015) determined an elevation-threshold, below/above which temperature/precipitation mainly controls the snowpack. Hantel et al., (2000) discussed the links of temperature and SCD, sensitivity of the latter under temperature change and described the most temperature-sensitive elevations for Austria, as well as seasonal differences thereof. These latter studies were conducted on either coarse resolution model outputs or point measurements and thus provide a more general picture.

In this study, we will apply the RSLE method as a means of large-scale cloud cover reduction for the estimation of D_{sc} from the MOD10A1 snow cover product across the GAR. The overall objective of this study is to, for the first time, provide a detailed, exclusively data-based documentation and analysis of regional differences in D_{sc} and its sensitivity to changes in temperature and precipitation beyond the catchment-scale. We will test the hypotheses that (1) there are spatial differences in temporal trends of D_{sc} throughout the GAR for the 2000-2017 study period and that (2) these differences can be quantitatively linked to spatially varying interactions between temperature and precipitation.

2. Study Domain

Our study domain includes the alpine mountain range, with the countries Austria, Slovenia, and Switzerland, as well as large parts of Italy, Bosnia, Croatia, Hungary, Slovakia, Czech Republic, Germany and France. In the literature, this part of Europe is often referred to as the GAR. The domain covers around 900 000km² and elevations range from -10 to 4810 m.a.s.l. The alpine arc itself stretches over 1200km from the Ligurian Sea to the Pannonian Basin. With its main ridge running east to west and south from there, it constitutes a natural climate and water divide. Major river basins in the GAR are Danube, Rhine, Rhone and Po. Alpine water thus drains into the Black, Northern, Mediterranean and Adriatic Seas. The forest line occurs at elevations of around 2000 m.a.s.l., the tree line between 2500 and 3000 m.a.s.l.. (Formayer and Nadeem, 2012) computed seasonal snowline elevations for the GAR. They assessed mean seasonal values ranging from 500 to 3100m.a.s.l., and large regional differences. Based on their results, they differentiated the domain into four sub-regions (Tab.1 and Fig.1, right panel). Another differentiation of the GAR, based on principle regional differences of climate elements (Fig.2), was undertaken by (Auer et al., 2006). Features show similarities to the snowline-differentiation above, especially along the main alpine ridge.

Subregion	Mean winter (DJF) snow line elevation (m.a.s.l.)	Colour in Fig. 1 (right panel)
Continental	~700	magenta
Atlantic/continental	~1100	blue
Mediterranean/continental	~1000	green
Maritime	~1500	Red

Tab. 1 Differentiation of the GAR into snowline/climatic subregions (Formayer and Nadeem, 2012)

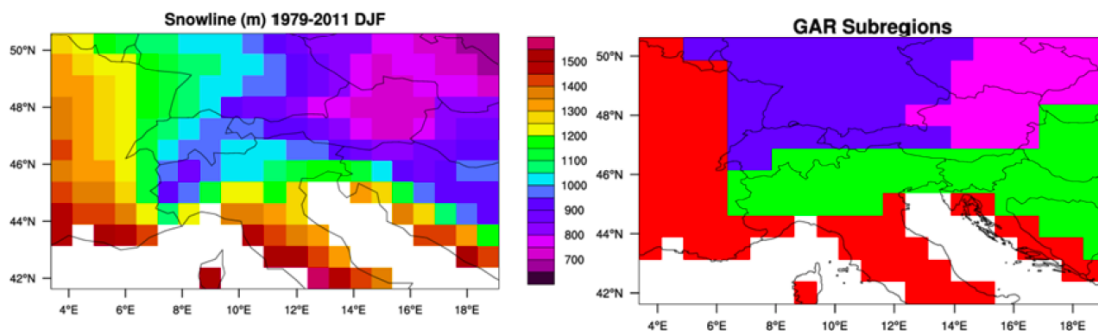


Fig. 1 Mean snow line elevation (left) and differentiation of the GAR into snowline/climatic subregions (right, Formayer and Nadeem, 2012)

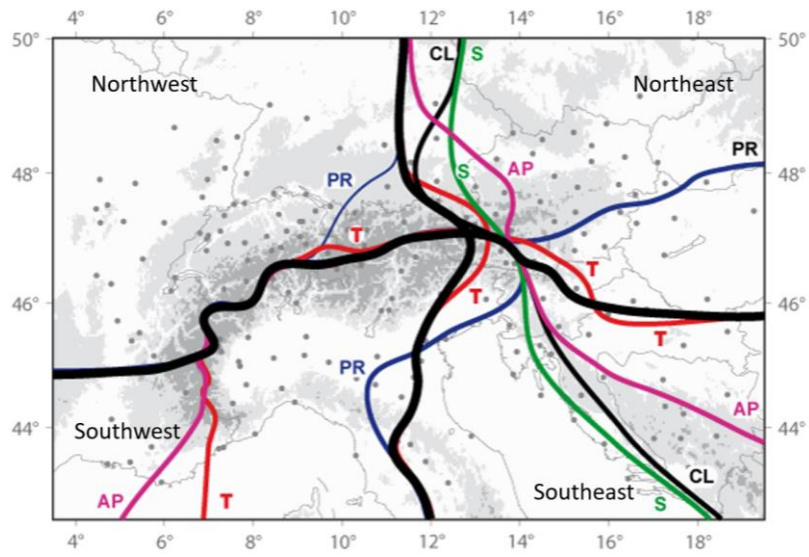


Fig. 2 Leading horizontal climatic sub-regions of the Greater Alpine Region (Auer et al., 2007);
 AP-air pressure, T-temperatur, PR-precipitation, S-sunshine duration, CL-cloudiness;

3. Data & Methods

MODIS Snow cover product MOD10A1, Version 6

Two NASA earth observation satellites (Aqua and Terra) carry the Moderate-resolution Imaging Spectroradiometer (MODIS). MODIS delivers remote sensing imagery consisting of 36 spectral bands covering wavelengths from 0,4 to 14,4 μm . With a daily revisit, it is meant to provide data for large-scale observation and analysis of land cover changes.

(Hall & Riggs, 2016) used a snow detection algorithm to assess the normalized difference snow index (NDSI) for the best observation per day and released a 500 by 500m snow cover product for each of the MODIS-carrying satellites, namely MOD10A1 (Terra) and MYD10A1 (Aqua). It is openly available, updated daily and distributed by the US National Snow and Ice Data Center (NSIDC). For this study, the MOD10A1 (Version 6) NDSI_Snow_Cover layers of parts h18v04 and h19v04 were used to compute snowline elevations. Besides gridded NDSI values ranging from 0 to 100, the layers contain classes for cloud, missing data, inland water, etc.

EU-DEM V1.1

The EU-DEM is a 25m Digital Surface Model provided by the European Environmental Agency (EEA, www.eea.europa.eu). For assessing the snowline elevations, the DEM parts E30N20 and E40N20 were merged, re-projected to the MGI/Austria Lambert coordinate reference system and (mean-)aggregated to the MODIS snow cover product resolution (500m).

Snow depth station data

Daily station measurements of vertical snow depth for Austria were used to compare MODIS-derived results of D_{sc} . Time series are differing in length, in the range between Sept. 1, 1970 and Sept. 1, 2014. Snow depth below 0.5cm was recorded as 0cm. The data is openly available from the Austrian hydrographical online database (eHyd, ehyd.gv.at).

SPARTACUS temperature and precipitation

This is a gridded (1km) dataset of daily minimum and maximum temperature (Hiebl & Frei, 2016) and daily precipitation sum (Hiebl & Frei, 2018), covering the period 1961 to present and is distributed by the Zentralanstalt für Meteorologie und Geodynamik (ZAMG, www.zamg.ac.at). It was used to identify temperature and precipitation as possible drivers for D_{sc} and changes thereof for the period 2000-2017.

3.1. Regional snow line elevation (RSLE)

Preparation of MODIS snow cover maps

Daily parts (h18v04 and h19v04) of the NDSI_Snow_Cover layers representing the period 25.02.2000 - 31.12.2017, i.e. 6450 days, were spatially merged, re-projected to the MGI/Austria Lambert coordinate reference system and cropped to the GAR domain. Quality check resulted in 30 rejects, dating mainly to the earlier days of MODIS recordings. The accepted layers were reclassified to contain 4 classes of pixels, i.e. “snow”, “land”, “cloud” and “no data“. A minimum snow-detection threshold of $NDSI = 0.4$ was used to differentiate between snow/land throughout the study domain, which Härer et al. (2017) considered as adequate at resolutions of 500m and above.

RSLE method

The RSLE method (Krajci & et.al., 2014) is a way to determine the average snow line elevation from partially cloud-obscured raster imagery for a given region, which may be a catchment or any other spatial domain of interest and suitable size. In its core part, the algorithm loops from the lowest to the highest DEM elevation within the chosen region by an elevation step of choice and minimizes a snow/land scatter value Sc_i , which is calculated as

$$Sc_i(h_i, t) = n_{s,b,h_i}(t) + n_{l,a,h_i}(t)$$

where n_{s,b,h_i} [-] and n_{l,a,h_i} [-] are the respective numbers of snow pixels below and land pixels above h_i in the region of interest. The elevation, at which the lowest value of Sc_i is found, is then defined as the regional snow line elevation (RSLE) for the time step. For a more detailed description of the method, the reader is referred to (Krajci et al., 2014). The assumption here is, that the natural variability of snow line elevation within the chosen region stays within an acceptable range. The larger the area, the larger that natural variability will be. Besides the region sizes, one must also consider the acceptable percentage of cloud cover over the area: Which share of it needs to be still visible to determine the RSLE in a reasonable way?

As this study applies the RSLE method on MODIS snow cover imagery to determine trends and spatial patterns of change for a large area (i.e. the GAR), a reasonable way to split into ‘snow line regions’ (hereafter referred to as ‘tiles’) had to be found. This leads into an optimization problem with the variables tile size and accepted share of cloud covered pixels in a tile on a given day (cloud cover threshold). Snow line estimation accuracy, index of scatter, resulting number of available days and computation time can thereby serve as objective criteria. This or a similar kind of optimization should be looked at before applying the RSLE method, to ensure that the accuracy of RSLE determined under presence of cloud cover meet required accuracy levels. The choice of tile-size in this study was based on a simple, preliminary sensitivity analysis: Tiles varying in size j from 20x20 pixels up to 120x120 pixels were generated for the study domain and daily RSLEs were calculated for the year 2001, allowing

for a maximum cloud cover of 70%. For the individual tiles of size j the following index of scatter $I_{s,j}$ [-] was then computed

$$I_{s,j}(t) = \frac{n_{s,b,RSLE,j}(t) + n_{l,a,RSLE,j}(t)}{A_j}$$

where $n_{s,b,RSLE,j}$ [-] and $n_{l,a,RSLE,j}$ [-] are the respective numbers of snow pixels below and land pixels above the RSLE in a specific tile of size j , A_j [-] is the total number of pixels for a tile of a specific size j , thus representing the area of the region under consideration. In a next step, the mean index of scatter $I_{s,j,mean}$ was computed for all days of the year 2001 with successful RSLE determination, limited to 100 randomly chosen tiles from throughout the study domain. As a balanced compromise between spatial variability of snow line, index of scatter and computation time, a tile-size of 50 by 50 pixels was chosen for this study (Fig. 3). Keeping the cloud cover threshold at 70% and introducing an additional minimum snow detection threshold of 1% (min. 1% snow covered pixels in a tile on a given day for RSLE calculation), to avoid small scale misclassifications, RSLE time series were now calculated for the whole study period.

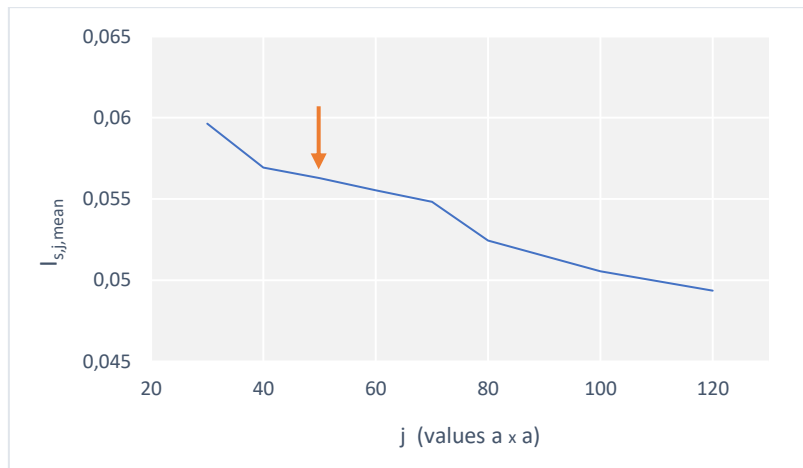


Fig. 3 Sensitivity of mean index of scatter to tile size

RSLE filtering

Visual control of snow line graphs revealed the presence of unrealistic spikes. These errors were filtered out, if consisting on a single value and if a certain difference in magnitude to the prior and the following day was identified:

$$RSLE(t) = \begin{cases} RSLE_{raw}(t), & |RSLE_{raw}(t) - RSLE_{raw}(t-1)| - |RSLE_{raw}(t+1) - RSLE_{raw}(t-1)| \leq \Delta RSLE_{crit} \\ "no data", & |RSLE_{raw}(t) - RSLE_{raw}(t-1)| - |RSLE_{raw}(t+1) - RSLE_{raw}(t-1)| > \Delta RSLE_{crit} \end{cases}$$

where $\Delta\text{RSLE}_{\text{crit}}$ is a maximum allowable difference of RSLE values at specific time steps t to the respective values at the prior, i.e. $t-1$, and the following time steps, i.e. $t+1$. In an iterative and explorative process $\Delta\text{RSLE}_{\text{crit}}$ was set to 700m in this study. When declared as “no data”, a gap was added to the already existing gaps stemming from cloud cover percentages above threshold or observation failures. Linear interpolation was applied for a maximum continuous gap of 8 days in a first step, while for the time being preserving days declared as non-snow-covered (‘land’) as well cloud-days between snow-covered and ‘land’-declared time steps. The resulting product served as the baseline for further analysis. For the calculation of D_{sc} , a continuous 365/366 days snowline was required. Therefore, earlier as ‘land’ declared tiles were set to maximum DEM-elevation (as if the snowline was at the highest possible elevation) and a second step of linear interpolation was applied for all remaining missing daily values. Linear temporal interpolation of snowline does not only serve as a simple way of closing these observation gaps but is based on the meaningful assumption of a gradually upwards- or downwards- moving snowline between successful observations.

Visualization of snow line time series

‘Raw’ RSLE time series of individual tiles would be difficult to interpret as they provide a rather fuzzy picture. For a meaningful visualization, aggregation was undertaken in three steps for (Fig. R1 to Fig. R4):

- Mean daily values for lumped tiles of regions of interest
- Calculation of monthly mean
- Rolling mean with a width of four years across inter-annual values

3.2. Influence of exposure to solar radiation

To learn about the influence of topography-exposure to solar radiation on RSLE, and to evaluate possible trends thereof, topography-sensitive, incoming solar radiation sum, calculated for two-week-time steps using the ‘Area Solar Radiation’ ArcGIS Spatial Analyst tool (Fu and Rich, 2002), was used to differentiate the landscape into two classes: Areas receiving sums above and below the median value. The RSLEs were now calculated twice per tile, respectively. To answer the question, whether solar exposure matters with regards to the trends in D_{sc} , three types of values were calculated and compared for the period 2000 to 2017 on a limited set of tiles, as indicated in (Fig.4):

- Change in mean monthly snow line elevation for high exposure
- Change in mean monthly snow line elevation for low exposure
- Change in the difference between the mean monthly snowline elevations for high/low exposure



Fig. 4 Limited set of tiles for the analysis on the influence of topography-exposure to solar radiation, snow line elevation and related trends;

3.3. Annual number of days snow covered (D_{sc})

Based on the gap-free RSLE time series for each tile for the period Feb. 2000 to Dec. 2017, the estimation of D_{sc} was performed. To capture the whole annual accumulation and melt cycle, the periods for the estimation of D_{sc} were here defined as August 16 to August 15 of the following year (hereafter ‘snow year’). D_{sc} varies greatly across the elevation profile. For a thorough assessment and subsequent trend analysis, now also the elevation profile was split into zones. A 100m elevation step was chosen, which seemed to stand in a good relation to natural variability of the snow line within the 625km² tile and the DEM resolution of 500m. To derive D_{sc} for those elevation zones, the area above snow line (-plot) was calculated from the time series as (see also Fig.5)

$$D_{sc,RSLE,k} = \sum_{t=1}^n \left(h_{t,k} + \frac{h_{t+1,k} - h_{t,k}}{2} \right) / 100$$

where $h_{t,k}$ is, for a given time step, the elevation difference between the maximum elevation of an elevation zone k and the RSLE, or the entire height of the elevation zone.

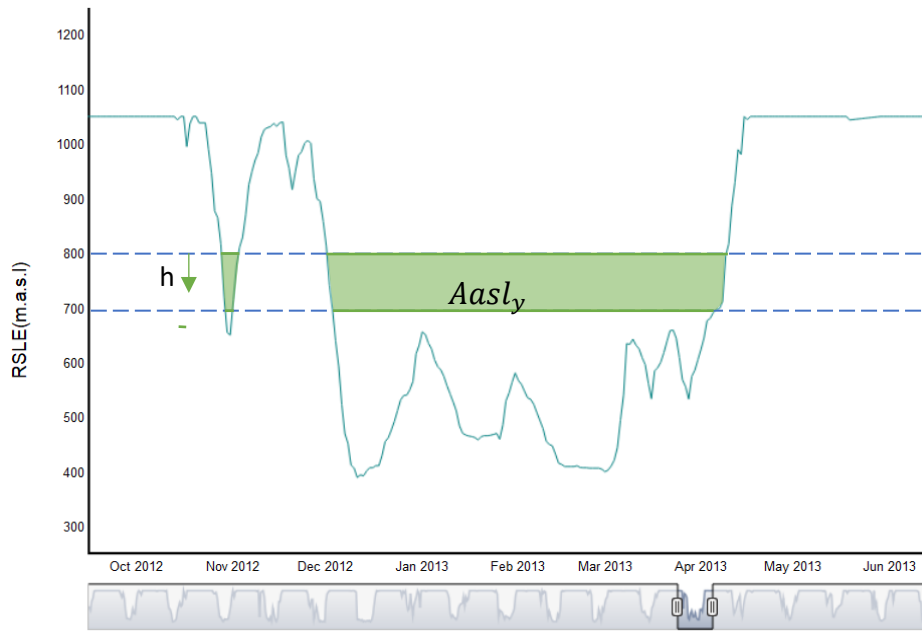


Fig. 5 Calculating annual SCD for one elevation zone; green shaded area is the 'area above snow line'

Comparison to ground station data

As a plausibility-check of RSLE- and thus MODIS-derived D_{sc} results, they were compared to D_{sc} derived from long-term point scale snow depth data from several observation stations in Austria. This also allowed for considering the relatively short MODIS derived trends of D_{sc} in a long-term perspective. Tiles and elevations were chosen with respect to geographical location and station data availability. Station D_{sc} were assessed for each snow year by counting the number of station measurements >0 cm only. Because mean regional (MODIS derived) values had to be compared to point measurement, the elevation of chosen slices was partly adjusted by ± 100 m. Anomalies were calculated for the combined time series based on station data mean for the period 1970 to 2000. From 2000 onwards, MODIS derived D_{sc} anomalies based on station mean, were plotted.

3.4. Trend analysis

A simple linear model was fitted to the MODIS derived D_{sc} time series.

$$D_{sc}(t) = I + \beta * t + \varepsilon$$

The slope β was thereby used to calculate a change in snow covered duration as

$$\Delta D_{sc} = \beta * (t_{max} - t_{min})$$

The p-value in comparison to significance level $\alpha = 0.05$ was used to determine whether a trend was significant.

$$\begin{aligned} \text{sign.} & \quad p \leq \alpha \\ \text{not sign.} & \quad p > \alpha \end{aligned}$$

Visualization of D_{sc} trends

To enhance the resolution of snowline outputs and for gaining a smoother picture, the RSLE method was applied on two overlapping sets of tiles, with a spatial offset of 25 pixels in two directions. Map results contain the mean of both sets. Maps were created by ‘replacing’ DEM elevation zones with ΔD_{sc} values.

3.5. Relating D_{sc} to temperature and precipitation

To identify dominant drivers of D_{sc} throughout the different elevation-zones, temperature and precipitation data had to be prepared to match the structure of D_{sc} results: From the min. and max. daily temperature of the SPARTACUS data set, the mean was calculated for each day. Mean winter temperature (wT) was then calculated for the period Nov.1 until Apr.30 - following year.

Precipitation was split into liquid and solid shares, as for the regressions, only solid precipitation would be of interest. This was done by using a binary 0°C mean daily temperature threshold, below which precipitation was assumed to fall as snow. The cumulative sum (csP) for entire years (Aug. 16 – Aug.15 -following year) was calculated and the results were split into elevation zones.

Linear trends in wT and csP for the SPARTACUS-period (1961-2017) and the MODIS-period (2000-2017) were calculated based on the 1km-grid. Next, mean yearly wT- and csP - grids were split to (RSLE-)tile extent and into 100m elevation zones. With the resulting data structure (Fig. 6), values of D_{sc} could now be related to their corresponding wT and csP.

			2000	
			2001	
			2002	
Elev.	Tile 55	Tile 56		
...	wT csP SCD	wT csP SCD		
700m	wT csP SCD	wT csP SCD		
600m	wT csP SCD	wT csP SCD		
500m	wT csP SCD	wT csP SCD		
...	wT csP SCD	wT csP SCD		

Fig. 6 data structure for regression analysis

Two simple linear regression models were set up, relating D_{sc} to wT and to the csP , respectively. Additionally, a multiple linear regression model was used to relate D_{sc} to both climate elements.

Simple linear regression:

$$SCD(t) = I + \beta_1 * wT(t) + \varepsilon$$

$$SCD(t) = I + \beta_1 * csP(t) + \varepsilon$$

Multiple linear regression:

$$SCD(t) = I + \beta_1 * wT(t) + \beta_2 * csP(t) + \varepsilon$$

The latter might contain auto-correlation, as solid precipitation was derived using threshold-temperature, results shall therefore be considered with caution. As evaluation metric, the adjusted R^2 , that accounts for the different numbers of explanatory variables was calculated for each tile and elevation zone.

$$R^2_{adj} = 1 - \left[\frac{(1 - R^2) * (n - 1)}{n - k - 1} \right]$$

where n is the number of observations and k is the number of predictor variables. In contrast to R^2 , R^2_{adj} can become negative when n is too low compared to k .

For the visualization of regression results, R^2_{adj} was plotted for regionally grouped tiles and elevation zones into boxplots. Grouping was done with respect to the patterns of change and corresponding climatic sub-regions (Fig. 2).

4. Results

(Figs. R1 to R22 are to be found in the Appendix Results)

4.1. Regional snow line elevation (RSLE)

To gain an insight into the yearly snow accumulation and melt dynamics as well as possible temporal shifts during the period 2000-2017, aggregated annual RSLEs were analysed (Fig. R1 to R3). A common feature for all regions is, that spring snowlines plot smoother compared to autumn snowlines. In Vorarlberg/Graubünden, Central Austria and Carinthia (Fig. R1 to R3, upper panels), RSLEs of more recent years tend to plot higher in elevation during spring, which indicates that snowmelt happens earlier. The date, when spring/autumn snowlines cross certain elevations are visualized in (Fig. R1 to R3, middle and lower panel). While autumn snowline crossings show a rather scattered picture, for spring, they plot with a tendency towards a shorter winter season, by the magnitude of 10 to 15 days. There are no such tendencies for Southern Tyrol (Fig. R4).

4.2. Influence of exposure to solar radiation

Long-term monthly mean RSLEs on terrain with a higher exposure to solar radiation plot higher throughout the year compared to terrain with lower exposure (Fig. R5). Differences, which reach values of up to 500m tend to be strongest in accumulation/depletion periods and during summer months. Monthly trends in snowline elevation at different exposures (Fig. R6 and R7) for the period 2000 to 2017 show some degree of spatial correlation, which indicates similar trends in RSLE across the chosen set of tiles. On the contrary, monthly trends in the difference between RSLE for the two exposure classes for the same period (Fig. R8) appear to be more scattered and random, which indicates the absence of coherent trends throughout the set. This implies.

4.3. Annual number of days snow covered (D_{sc})

Comparing MODIS derived D_{sc} to days with snow depth >0cm at individual ground measurement stations (Fig.R9 to R14) shows good agreement in both, variation and magnitude, at lower (e.g. Sopron, 300m, Fig.R13) as well as at higher elevations (e.g. St.Anton am Arlberg, 1700m, Fig.R10). This indicates, that the method performs well and that the level of accuracy suits the scale of problem under consideration.

Attention should also be paid to the variability of D_{sc} : Interannual variabilities on average are stronger in lower, compared to higher areas. This may bear implications for the significance of

trends. It also demonstrates that one or several short-term trends can be embedded in a long-term trend pointing towards the opposite direction (e.g. Sopron).

Anomalies give an insight on how D_{sc} varies throughout the years compared to the long-term mean. Negative anomalies indicate a systematically lower D_{sc} in more recent years at four out of six locations (St. Anton, Innervillgraten, Nockberge, Zugspitze) and especially pronounced anomalies (e.g. Innervillgraten, up to -75 days) in the MODIS-covered period for most sites. At the Sopron and Bad Aussee area, the picture is less clear.

4.4. Trend analysis

Plotting results from trend analysis on D_{sc} derived from RSLEs on top of a GAR map allows for seeing patterns of change throughout the domain. The resulting picture appears to be relatively consistent, with gradations of D_{sc} change magnitudes. However, breaks at the boundaries of tiles are still clearly visible (Fig. R15), which are artefacts originating in the tile-based calculation of snowlines. Highest values of change (up to -35 days change) are found in the lower regions of the north-eastern and eastern GAR, as well as at higher elevations in the Austrian, Swiss and Italian Alps. In some regions, e.g. parts of Carinthia, Salzburg or Vorarlberg, we see no trends or weak positive trends below 1500m (0 to +10 days change). Considering only the alpine arc in general, the image seems to be more differentiated at the south-, compared to north side of the main alpine ridge. Tiles with significant trends (Fig. R16 to R18) appear to be relatively scattered at lower elevations, mostly throughout the north-eastern GAR and range between -5 and -35 days of change. At higher elevations, most of them concentrate in the alps, throughout Austria, Switzerland and France, north of the main alpine ridge, between 1200 and 3400m.a.s.l.

Trends of short-term wT (Fig. R19) for Austria range between +1°C and +1.8°C and are stronger at higher elevations. Particularly strong trends appear in the eastern-most parts of the alps. Interestingly, long-term trends of wT, ranging between +2.2°C and 3.0°C, do not show this behaviour. For both periods, there is no pattern related to the horizontal climatic sub-regions, as far as it can be told from the limited coverage of dataset at hand. Both, short- and long-term negative trends of cumulative csP are stronger (short-term: up to -200mm, long-term: up to -400mm) at higher elevations in large parts of the domain. However, short-term trends also show an increase in csP by up to 50mm for parts of Southern Austria, especially the parts coinciding with the south-eastern climatic sub-region (Carinthia) as defined by Auer et al. (2006).

4.5. Relating D_{sc} to temperature and precipitation

To move on to the combined analysis of D_{sc} with climate elements (Fig. R20 to R22), grouped with respect to climatic sub-regions, regression results illustrated as boxplots show that at lower and higher elevations, up to 75% of D_{sc} variability can be explained by either wT or csP. Around

2000 m.a.s.l., R^2_{adj} -values drop to their lowest values, some of them even become negative, which is to interpret as 0. North of the main alpine ridge and at moderate elevations (around 500-1500 m.a.s.l.), wT appears to be controlling D_{sc} (wT up to 75% vs. csP up to 60%) while south, csP outperforms wT as explanatory variable (wT up to 30% vs. csP up to 65%). Above 2000 m.a.s.l., csP strongly outperforms wT in all regions (eg. Vorarlberg/Tirol, wT around 0% vs. csP up to 50%).

5. Discussion

Temporal changes and regional patterns

Considering plots of RSLE time series at a suitable level of aggregation (Fig. R1 and R4), seasonal differences of snow cover evolution become visible, which can be related to what is happening in the field: spring snowline shows a smoother evolution than autumn snowline. This is due to a variable, event-based snow cover onset in autumn and a more gradual snow cover depletion in spring. But also signals of change (over the years) can be visually determined. More recent snow lines plot higher up, especially north of the main alpine ridge, which translates into a shorter period of snow cover at affected elevations. These short-term declining trends embed well into long-term trends assessed for Switzerland by Klein et al. (2016) and, taking D_{sc} as a proxy for SWE, also agree to the results of Marty et al. (2017b). The results for the Schladming area assessed by Marke et al. (2015) for the period 2021 to 2050 predict a further decrease in D_{sc} by average decrease rates of 2.6 d yr^{-1} , while our observations for 2000-2017 are in the range of (i.e. $\sim 1 \text{ d yr}^{-1}$).

Considering results of the trend analysis (Fig. R15) in detail, hypothesis (1) can be answered with “yes”- there are large regional differences in the change of D_{sc} , however, there are at least as large differences connected to elevation. Regarding the significance of trends (Fig. R16 to R18), results may be relativized, when again considering interannual variabilities in (Fig. R9 to R14): The larger the variance, as it is the case at lower elevations, the lower the significance-levels will be.

Effects of exposure

Snowline elevations show systematic monthly differences between areas with low/high solar radiation inputs. While this differentiation is potentially interesting for applications including e.g. hydrological modelling, we do not see a necessity to further include it for the analysis on D_{sc} . This is because we do not find considerable trends in the difference between the two classes. We thereby assume that each of the 625km^2 tiles contains a fair share of all exposure, and thus, mean values of snowline elevation contain sufficient information on the trends.

Temperature and Precipitation as drivers

The climate elements wT and csP controlling D_{sc} at lower/higher elevations reflect well what was found by (Sospedra-Alfonso et al., 2015). However, explanatory power of the two and their combination seem to vary greatly across elevations. Especially at elevations around 2000m.a.s.l. where explanatory power drops to zero, there must be mechanisms in control which are not captured by our simple D_{sc} -temperature-precipitation-model: Results may be influenced by biases in the SPARTACUS dataset. Most temperature/precipitation measurements are carried out at low to moderate elevations, while grid estimates at higher

elevation reflect mostly modelled results. Another source of uncertainty is connected to the binary temperature-threshold used for estimating solid precipitation from total precipitation. More sophisticated methods to estimate rain-snow transition include dewpoint temperature or wet bulb temperature (Marks et al., 2013), however, the therefore necessary datasets are not available at the required scale. Finally, we were so far only dealing with snow cover distribution in three dimensions, yet there is a fourth dimension: the storage dimension or SWE. In the following, a short interpretation of the regression results, with respect to the storage is given: At elevations below 1500m.a.s.l., snow onset and melt-out happens several times during a season. Thus, from space, we see a sequence of covered/non-covered periods. The wT/csP – time series can explain the length of these sub-periods and thus the total D_{sc} during a year. Higher up, around 2000m.a.s.l., a continuous snow cover is expected throughout the season in contrast to the lower elevations. But still, temperatures can rise well above 0°C and considerable depletion/accumulation processes are happening during the season. The difference compared to lower regions is, that those processes cannot be captured with optical remote sensing. In other words, we are ‘blind’ regarding to what is happening with the storage at those elevations. At the same time, the date of snow cover onset plays a decisive part, which itself is controlled by a sensitive interplay between the temperature of arriving air masses and precipitation events (Hantel et al., 2000). On the contrary, higher up, a continuous snow cover is subject to mostly accumulation processes, as temperatures are low throughout the season. Any precipitation accumulates and stays until the major snowmelt-events in spring. Thus, csP succeeds to explain large shares of D_{sc} variability at those elevations.

While these relationships could potentially inform about the power and limitations of snow cover remote sensing, ways to back them up empirically are rather limited, mainly due to the absence or low quality of SWE data.

Linking changes, regional patterns and controls

Three issues raise the question of how climatic elements control the changes we see, including their regional patterns:

(a) There is a presence/lack of significant trends, at similar elevations, north/south of the main alpine ridge. They align with snowline- and climatic sub-regions (Auer et al., 2006; Formayer and Nadeem, 2012). (b) Trends in csP show partly opposing trends for different climatic sub-regions. (c) Regression results show opposing behaviours for the same regions.

Most results of D_{sc} for Austria show a clear, yet less informative picture: Higher temperatures - less snowfall - less D_{sc} , at all elevations. On the contrary, regions like Carinthia or parts of Salzburg and Vorarlberg are more differentiated: At lower elevations, minor to no declines, or minor increases of D_{sc} are observable together with an increase in csP. But especially elevations above 1500m show a strong decline in D_{sc} , even where short-term csP increased, and csP at the same time has more explanatory power. A possible explanation is, that increases in wT offset higher csP at most elevations, in other words, average warming causes a shortening of the snow-covered season, regardless of the snowfall amounts. This would be in agreement with findings of Mankin and Duffenbaugh (2015) and Räisänen (2008): Despite higher values of modelled

SWE for some regions during high winter, the snow season shortens, which can be attributed to later/earlier snow accumulation/depletion due to a temperature rise.

However, the question connected to hypothesis (2), i.e. how regional differences in the change of D_{sc} can be linked to spatially varying interactions between temperature and precipitation, can only partly be answered in this study and remains open to further research.

On the method

Working with RSLEs has clear advantages over snow mapping techniques dealing with two-dimensional spatial patterns: By incorporating the third dimension (in the form of a DEM), a variable with strong links to the natural processes of snow cover distribution, more specifically – a rising and descending snow line due to melt and accumulation, is added. Another strength comes with the implicit reduction of cloud obscuration when applying the method. Finally, many elements describing spatio-temporal snow cover distribution, including the snow line elevation itself, can be derived directly from resulting time series. However, the RSLE needs to be considered merely as a proxy value for the natural - due to factors like exposure, meso-climate, preferential accumulation, snow deposition - highly variable snow line, as it is, by definition, an average value for a pre-defined region, with the minimum scatter $SC_{i,min}$ as primary assessment-criterion.

There is another assumption, which will certainly not always be fulfilled on the ground: All area above the snowline is snow-covered, all area below is not snow-covered, while under natural conditions, snow cover often tends to be fractional. Areas should therefore rather be considered as ‘snow dominated’ or ‘not snow dominated’, adopting terminologies proposed by Allchin and Déry (2017).

These assumptions require, that the scale of the problem under consideration and accuracy-requirements need to be thought about carefully before choosing to apply the method. For example, accuracy-requirements for applications on a scale considerably below the chosen region size - be it a certain catchment - will probably not be fulfilled. (sub-catchment-scale hydrology, avalanche research, ...)

We find, that these requirements are met for our application, i.e. assessing and analysing yearly D_{sc} , as we succeed to derive comparable D_{sc} time series from MODIS and station data respectively (Fig.R9 to R14, upper panels). One must bear in mind, that point-information is being compared to mean regional values derived from a 500m grid for elevation-zones of 100m. For this comparison, we did not deal with factors like station exposure, snow drift or preferential deposition and MODIS-elevations were adjusted for comparison by +/-100m, yet agreements in terms of variation and magnitude are satisfying.

Further applications

Methods and datasets combined in this study perform well to describe the spatio-temporal distribution of snow cover. The approach can be used to map snow line and snow cover across

scales (catchment to global), on a daily time step. Considering further applications, it can serve as a spatially explicit extension to long-term station data allowing for studies on the effects of climate change on snow cover distribution. As a proxy for SWE, the snow cover extents can be used for the calibration of hydrological models. It can also provide valuable inputs for SWE modelling as well as studies involving albedo back-scattering as an element of the earth's energy-balance, or for the validation of snow cover outputs from RCMs and land surface models.

6. Conclusions

We applied the RSLE method on the MODIS snow cover product for the Greater Alpine Region, to analyse the dynamics of snow cover duration and regional patterns and changes thereof for the period 2000 to 2017, assessed the effect of exposure, compared our results to station data, linked our findings to gridded temperature and precipitation data and discussed further possible applications. We found that,

- The combination of methods performs well, the accuracy of data and method suit the scale of the problem under consideration;
- The methods can furthermore be used to differentiate between topographies of distinct solar radiation input for snow cover mapping;
- There are partly significant, mostly negative trends of D_{sc} throughout the GAR, acknowledging the fact, that high interannual variabilities of snow cover characteristics compromise significance levels, and that a time series of 17 winters is not long enough to be related to climate change effects - short-term trends happen to be embedded in long-term trends pointing into the opposite direction;
- Regional patterns of D_{sc} can be linked to wT and csP, however with limitations, as we cannot take the storage-dimension into account, due to an absence of respective datasets;
- Even in regions, where csP increased, we find reduction of D_{sc} across elevations;

Bibliography

- Allchin, M. I. and Déry, S. J.: A spatio-temporal analysis of trends in Northern Hemisphere snow-dominated area and duration, 1971–2014, *Ann. Glaciol.*, 58(75), 21–35, doi:10.1017/aog.2017.47, 2017.
- Andreadis, K. M. and Lettenmaier, D. P.: Assimilating remotely sensed snow observations into a macroscale hydrology model, *Adv. Water Resour.*, 29(6), 872–886, doi:10.1016/j.advwatres.2005.08.004, 2006.
- Auer, I., Bohm, R., Jurkovic, A. and Lipa, W.: HISTALP – historical instrumental climatological surface time series of the Greater Alpine Region, *Int. J. Climatol.*, 27, 17–46, doi:10.1002/joc.1377, 2006.
- Barnett, T., Adam, J. and Lettenmaier, D.: Potential impacts of a warming climate on water availability in snow-dominated regions, *Nature*, 438(7066), 303–309, doi:10.1038/nature04141, 2005.
- Beniston, M., Farinotti, D., Stoffel, M., Andreassen, L. M., Coppola, E., Eckert, N., Fantini, A., Giacona, F., Hauck, C., Huss, M., Huwald, H., Lehning, M., López-Moreno, J.-I., Magnusson, J., Marty, C., Terzago, S., Vincent, C. and Beniston martinbeniston, M.: The European mountain cryosphere: a review of its current state, trends, and future challenges, *Mohamed Naaim Antonello Provenzale Antoine Rabatel*, 12(18), 759–794, doi:10.5194/tc-12-759-2018, 2018.
- Berghuijs, W. R., Woods, R. A. and Hrachowitz, M.: A precipitation shift from snow towards rain leads to a decrease in streamflow, *Nat. Clim. Chang.*, 4(7), 583–586, doi:10.1038/nclimate2246, 2014.
- Crawford, C. J.: MODIS Terra Collection 6 fractional snow cover validation in mountainous terrain during spring snowmelt using Landsat TM and ETM+, *Hydrol. Process.*, doi:10.1002/hyp.10134, 2015.
- Déry, S. J. and Brown, R. D.: Recent Northern Hemisphere snow cover extent trends and implications for the snow-albedo feedback, *Geophys. Res. Lett.*, 34(22), 2–7, doi:10.1029/2007GL031474, 2007.
- Dietz, A. J., Wohner, C. and Kuenzer, C.: European snow cover characteristics between 2000 and 2011 derived from improved modis daily snow cover products, *Remote Sens.*, 4(8), 2432–2454, doi:10.3390/rs4082432, 2012.
- Dong, C. and Menzel, L.: Producing cloud-free MODIS snow cover products with conditional probability interpolation and meteorological data, *Remote Sens. Environ.*, 186, 439–451, doi:10.1016/j.rse.2016.09.019, 2016.
- Durand, Y., Giraud, G., Laternser, M., Etchevers, P., Mérindol, L. and Lesaffre, B.: Reanalysis of 47 years of climate in the French Alps (1958–2005): Climatology and trends for snow cover, *J. Appl. Meteorol. Climatol.*, 48(12), 2487–2512, doi:10.1175/2009JAMC1810.1, 2009.
- Elsasser, H. and Bürki, R.: Climate change as a threat to tourism in the Alps, *Clim. Res.*, doi:10.3354/cr020253, 2002.
- Fernandes, R., Zhao, H., Wang, X., Key, J., Qu, X. and Hall, A.: Controls on Northern

Hemisphere snow albedo feedback quantified using satellite Earth observations, *Geophys. Res. Lett.*, 36(21), 1–7, doi:10.1029/2009GL040057, 2009.

Formayer, H. and Nadeem, I.: Klimatologie der Schneefallgrenze im Alpenraum, abgeleitet aus Reanalysedaten, , 26, 2012.

Fu, P. and Rich, P.: A geometric solar radiation model with applications in agriculture and forestry, *Comput. Electron. Agric.*, doi:10.1016/S0168-1699(02)00115-1, 2002.

Gafurov, A. and Bárdossy, A.: Cloud removal methodology from MODIS snow cover product, *Hydrol. Earth Syst. Sci.*, 13(7), 1361–1373, doi:10.5194/hess-13-1361-2009, 2009.

Gascoin, S., Hagolle, O., Huc, M., Jarlan, L., Dejoux, J. F., Szczypta, C., Marti, R. and Sánchez, R.: A snow cover climatology for the Pyrenees from MODIS snow products, *Hydrol. Earth Syst. Sci.*, 19(5), 2337–2351, doi:10.5194/hess-19-2337-2015, 2015.

Hall, D. K. and Riggs, G. A.: Accuracy assessment of the MODIS snow products, in *Hydrological Processes.*, 2007.

Hall, D. K., Riggs, G. A., Salomonson, V. V., Digirolamo, N. E. and Bayr, K. J.: MODIS snow-cover products, , 83, 181–194, 2002.

Hantel, M., Ehrendorfer, M. and Haslinger, A.: Climate sensitivity of snow cover duration in Austria, *Int. J. Climatol.*, 20(6), 615–640, doi:10.1002/(SICI)1097-0088(200005)20:6<615::AID-JOC489>3.0.CO;2-0, 2000.

Härer, S., Bernhardt, M., Siebers, M. and Schulz, K.: On the need of a time and location dependent estimation of the NDSI threshold value for reducing existing uncertainties in snow cover maps at different scales, *Cryosph.*, (under review), 1–27, doi:10.5194/tc-2017-177, 2017.

Hori, M., Sugiura, K., Kobayashi, K., Aoki, T., Tanikawa, T., Kuchiki, K., Niwano, M. and Enomoto, H.: A 38-year (1978–2015) Northern Hemisphere daily snow cover extent product derived using consistent objective criteria from satellite-borne optical sensors, *Remote Sens. Environ.*, 191, 402–418, doi:10.1016/j.rse.2017.01.023, 2017.

Hrachowitz, M., Savenije, H. H. G., Blöschl, G., McDonnell, J. J., Sivapalan, M., Pomeroy, J. W., Arheimer, B., Blume, T., Clark, M. P., Ehret, U., Fencica, F., Freer, J. E., Gelfan, A., Gupta, H. V., Hughes, D. a., Hut, R. W., Montanari, A., Pande, S., Tetzlaff, D., Troch, P. a., Uhlenbrook, S., Wagener, T., Winsemius, H. C., Woods, R. a., Zehe, E. and Cudennec, C.: A decade of Predictions in Ungauged Basins (PUB) - a review, *Hydrol. Sci. J.*, 58(6), 1198–1255, doi:10.1080/02626667.2013.803183, 2013.

Immerzeel, W. W., Droogers, P., de Jong, S. M. and Bierkens, M. F. P.: Large-scale monitoring of snow cover and runoff simulation in Himalayan river basins using remote sensing, *Remote Sens. Environ.*, 113(1), 40–49, doi:10.1016/j.rse.2008.08.010, 2009.

Jenicek, M., Seibert, J. and Staudinger, M.: Modeling of Future Changes in Seasonal Snowpack and Impacts on Summer Low Flows in Alpine Catchments, *Water Resour. Res.*, 54(1), 538–556, doi:10.1002/2017WR021648, 2018.

Klein, G., Vitasse, Y., Rixen, C., Marty, C. and Rebetez, M.: Shorter snow cover duration since 1970 in the swiss alps due to earlier snowmelt more than to later snow onset, *Clim. Change*, 139(3), 637–649, doi:10.1007/s10584-016-1806-y, 2016.

Krajci, P., Holko, L., Perdigg??o, R. A. P. and Parajka, J.: Estimation of regional snowline elevation (RSLE) from MODIS images for seasonally snow covered mountain basins, J.

- Hydrol., 519(PB), 1769–1778, doi:10.1016/j.jhydrol.2014.08.064, 2014.
- Krajčí, P., Holko, L. and Parajka, J.: Variability of snow line elevation, snow cover area and depletion in the main Slovak basins in winters 2001–2014, *J. Hydrol. Hydromechanics*, 64(1), 12–22, doi:10.1515/johh-2016-0011, 2016.
- Laaha, G., Parajka, J., Viglione, A., Koffler, D., Haslinger, K., Schöner, W., Zehetgruber, J. and Blöschl, G.: A three-pillar approach to assessing climate impacts on low flows, *Hydrol. Earth Syst. Sci.*, 20(9), 3967–3985, doi:10.5194/hess-20-3967-2016, 2016.
- Lehning, M., Löwe, H., Ryser, M. and Raderschall, N.: Inhomogeneous precipitation distribution and snow transport in steep terrain, *Water Resour. Res.*, 44(7), 1–19, doi:10.1029/2007WR006545, 2008.
- Madani, K. and Lund, J. R.: Estimated impacts of climate warming on California’s high-elevation hydropower, *Clim. Change*, doi:10.1007/s10584-009-9750-8, 2010.
- Mankin, J. S. and Diffenbaugh, N. S.: Influence of temperature and precipitation variability on near-term snow trends, *Clim. Dyn.*, 45(3–4), 1099–1116, doi:10.1007/s00382-014-2357-4, 2015.
- Mankin, J. S., Viviroli, D., Mesfin, M., Rastogi, D., Jennings, K. S. and Meier, J.: The potential for snow to supply human water demand in the present and future The potential for snow to supply human water demand in the present and future, *Environ. Res. Lett.*, 1–10, 2015.
- Marke, T., Strasser, U., Hanzer, F., Stötter, J., Wilcke, R. A. I. and Gobiet, A.: Scenarios of Future Snow Conditions in Styria (Austrian Alps), *J. Hydrometeorol.*, 16(1), 261–277, doi:10.1175/JHM-D-14-0035.1, 2015.
- Marks, D., Winstral, A., Reba, M., Pomeroy, J. and Kumar, M.: An evaluation of methods for determining during-storm precipitation phase and the rain/snow transition elevation at the surface in a mountain basin, *Adv. Water Resour.*, 55, 98–110, doi:10.1016/j.advwatres.2012.11.012, 2013.
- Marty, C.: Regime shift of snow days in Switzerland, *Geophys. Res. Lett.*, 35(12), 1–5, doi:10.1029/2008GL033998, 2008.
- Marty, C., Schögl, S., Bavay, M. and Lehning, M.: How much can we save? Impact of different emission scenarios on future snow cover in the Alps, *Cryosphere*, 11(1), 517–529, doi:10.5194/tc-11-517-2017, 2017a.
- Marty, C., Tilg, A.-M. and Jonas, T.: Recent Evidence of Large-Scale Receding Snow Water Equivalents in the European Alps, *J. Hydrometeorol.*, doi:10.1175/JHM-D-16-0188.1, 2017b.
- Marty, C., Tilg, A.-M. and Jonas, T.: Recent Evidence of Large-Scale Receding Snow Water Equivalents in the European Alps, *J. Hydrometeorol.*, 18(4), 1021–1031, doi:10.1175/JHM-D-16-0188.1, 2017c.
- Meißl, G., Formayer, H., Klebinder, K., Kerl, F., Schöberl, F., Geitner, C., Markart, G., Leidinger, D. and Bronstert, A.: Climate change effects on hydrological system conditions influencing generation of storm runoff in small Alpine catchments, *Hydrol. Process.*, 31(6), 1314–1330, doi:10.1002/hyp.11104, 2017.
- Molini, A., Katul, G. G. and Porporato, A.: Maximum discharge from snowmelt in a changing climate, *Geophys. Res. Lett.*, 38(5), 1–5, doi:10.1029/2010GL046477, 2011.

- Mudryk, L. R., Derksen, C., Kushner, P. J. and Brown, R.: Characterization of Northern Hemisphere snow water equivalent datasets, 1981-2010, *J. Clim.*, 28(20), 8037–8051, doi:10.1175/JCLI-D-15-0229.1, 2015.
- Nijzink, R. C.: Selecting model formulations and parameterizations: Reducing the need for calibration using open data and landscape characteristics, Delft University of Technology., 2018.
- Painter, T. H., Rittger, K., McKenzie, C., Slaughter, P., Davis, R. E. and Dozier, J.: Retrieval of subpixel snow covered area, grain size, and albedo from MODIS, *Remote Sens. Environ.*, doi:10.1016/j.rse.2009.01.001, 2009.
- Parajka, J. and Blöschl, G.: Validation of MODIS snow cover over Austria, , (March), 1–4, 2006.
- Parajka, J. and Blöschl, G.: Spatio-temporal combination of MODIS images - Potential for snow cover mapping, *Water Resour. Res.*, 44(3), 1–13, doi:10.1029/2007WR006204, 2008.
- Parajka, J., Kohnová, S., Bálint, G., Barbuc, M., Borga, M., Claps, P., Cheval, S., Dumitrescu, A., Gaume, E., Hlavčová, K., Merz, R., Pfaundler, M., Stancalie, G., Szolgay, J. and Blöschl, G.: Seasonal characteristics of flood regimes across the Alpine-Carpathian range, *J. Hydrol.*, 394(1–2), 78–89, doi:10.1016/j.jhydrol.2010.05.015, 2010.
- Parajka, J., Holko, L., Kostka, Z. and Blöschl, G.: MODIS snow cover mapping accuracy in a small mountain catchment - Comparison between open and forest sites, *Hydrol. Earth Syst. Sci.*, 16(7), 2365–2377, doi:10.5194/hess-16-2365-2012, 2012.
- Räisänen, J.: Warmer climate: Less or more snow?, *Clim. Dyn.*, 30(2–3), 307–319, doi:10.1007/s00382-007-0289-y, 2008.
- Rittger, K., Painter, T. H. and Dozier, J.: Assessment of methods for mapping snow cover from MODIS Author 's personal copy, *Adv. Sp. Res.*, 51, 367–380, 2013.
- Scherrer, S. C., Wüthrich, C., Croci-Maspoli, M., Weingartner, R. and Appenzeller, C.: Snow variability in the Swiss Alps 1864-2009, *Int. J. Climatol.*, 33(15), 3162–3173, doi:10.1002/joc.3653, 2013.
- Sospedra-Alfonso, R., Melton, J. R. and Merryfield, W. J.: Effects of temperature and precipitation on snowpack variability in the Central Rocky Mountains as a function of elevation, *Geophys. Res. Lett.*, 42(11), 4429–4438, doi:10.1002/2015GL063898, 2015.
- Stehr, A. and Aguayo, M.: Snow cover dynamics in Andean watersheds of Chile (32.0-39.5 degrees S) during the years 2000-2016, *Hydrol. Earth Syst. Sci.*, 21(10), 5111–5126, doi:10.5194/hess-21-5111-2017, 2017.
- Steiger, R. and Abegg, B.: Ski areas' competitiveness in the light of climate change: comparative analysis in the Eastern Alps, in *Tourism in Transition: Recovering decline, managing change.*, 2016.
- Tang, Z., Wang, J., Li, H. and Yan, L.: Spatiotemporal changes of snow cover over the Tibetan plateau based on cloud-removed moderate resolution imaging spectroradiometer fractional snow cover product from 2001 to 2011, *J. Appl. Remote Sens.*, 7(1), 073582, doi:10.1117/1.JRS.7.073582, 2013.
- Tomaszewska, M. A. and Henebry, G. M.: Changing snow seasonality in the highlands of Kyrgyzstan, *Environ. Res. Lett.*, 13(6), 065006, doi:10.1088/1748-9326/aabd6f, 2018.

Valt, M. and Cianfarra, P.: Recent snow cover variability in the Italian Alps, *Cold Reg. Sci. Technol.*, 64(2), 146–157, doi:10.1016/j.coldregions.2010.08.008, 2010.

Verfaillie, D., Lafaysse, M., Déqué, M., Eckert, N., Lejeune, Y. and Morin, S.: Multi-component ensembles of future meteorological and natural snow conditions for 1500 m altitude in the Chartreuse mountain range, Northern French Alps, *Cryosphere*, 12(4), 1249–1271, doi:10.5194/tc-12-1249-2018, 2018.

Appendix - Results

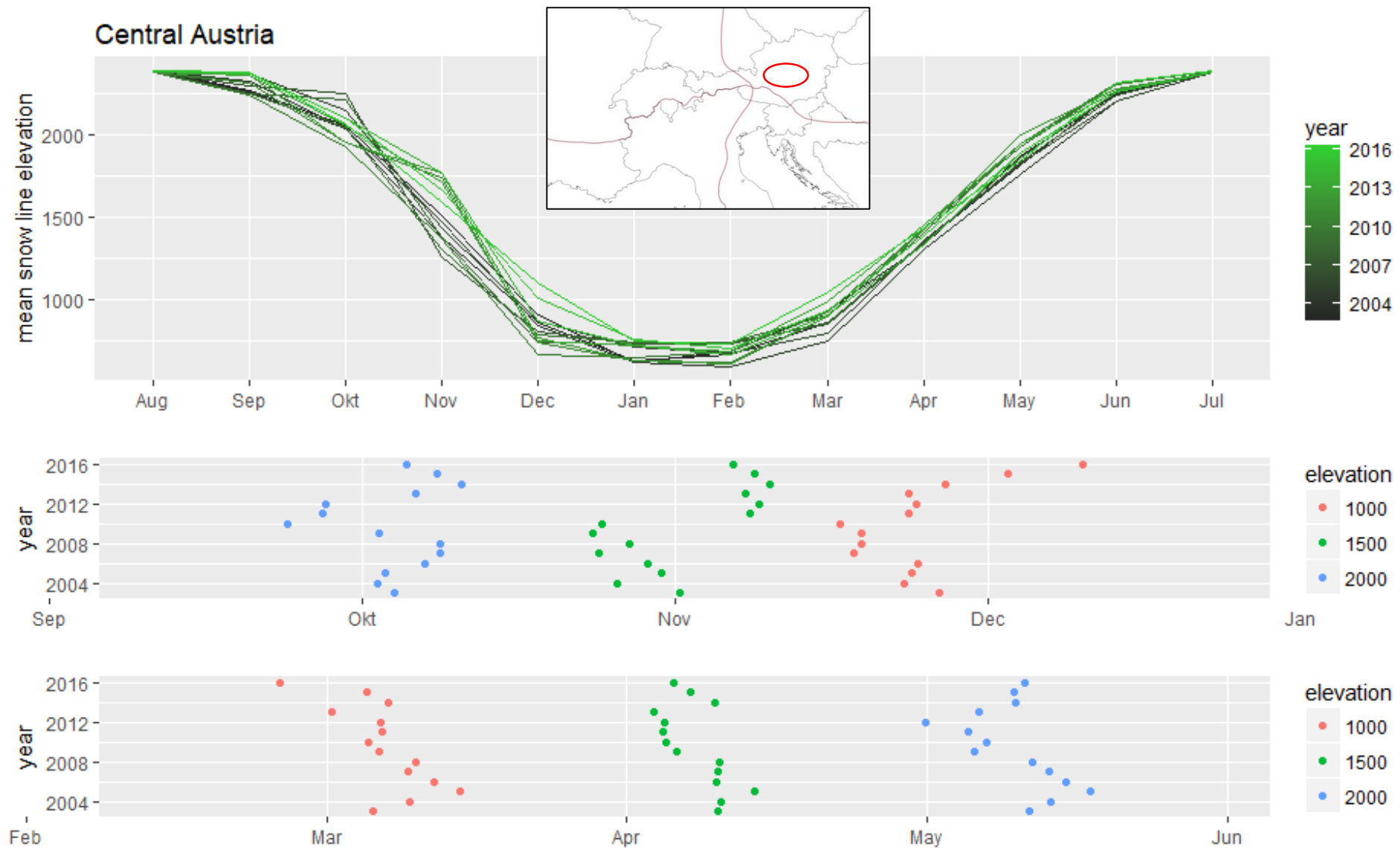


Fig. R1 upper panel: Average snowline elevations for tiles in Central Austria; monthly means per year; rolling mean with a width of 4 years was applied; middle and lower panel: dates of snowline 'crossing' selected elevations for autumn (middle) and spring (lower);

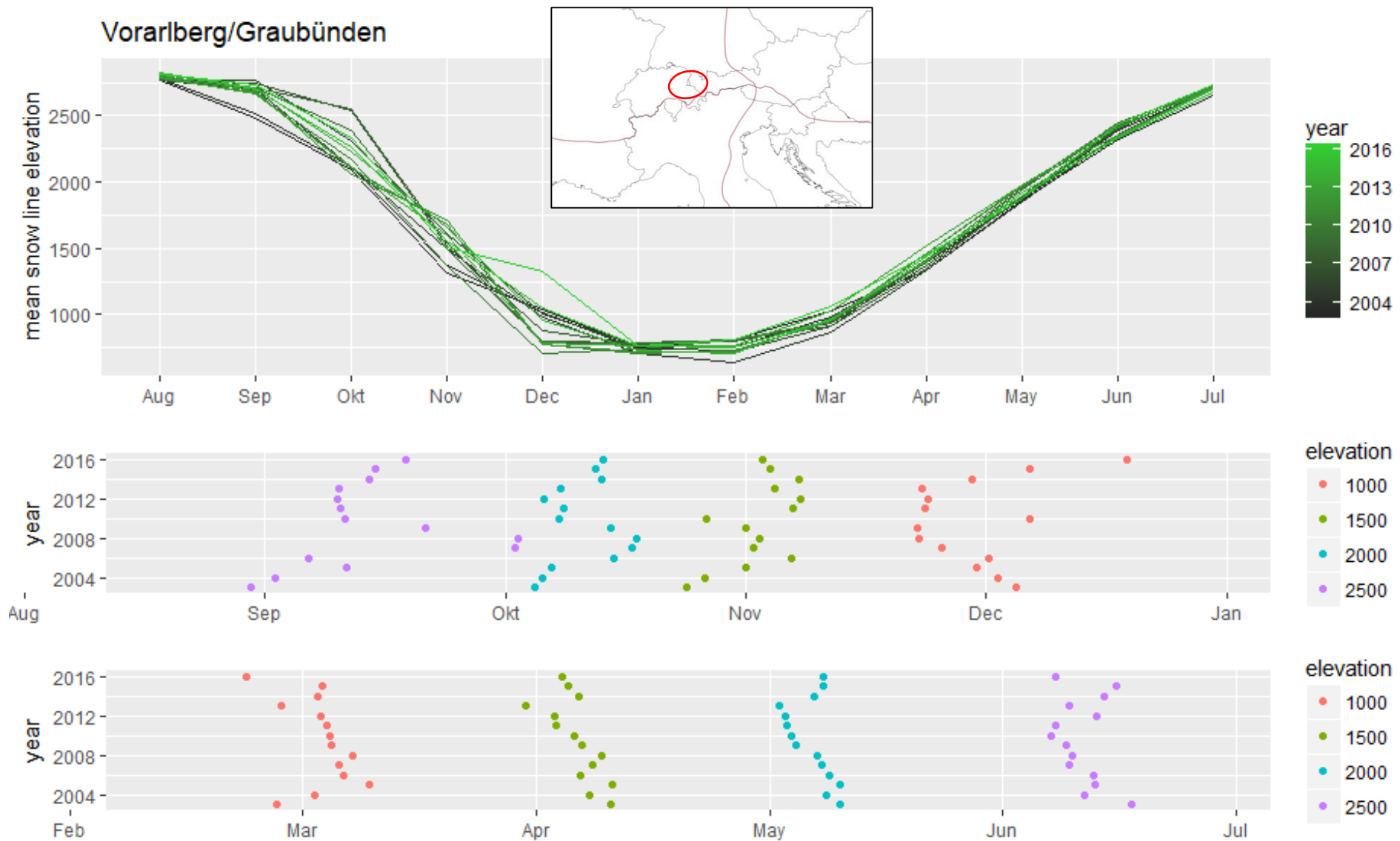


Fig. R2 upper panel: Average snowline elevations for tiles in Vorarlberg/Graubünden; monthly means per year; rolling mean with a width of 4 years was applied; middle and lower panel: dates of snowline ‘crossing’ selected elevations for autumn (middle) and spring (lower);

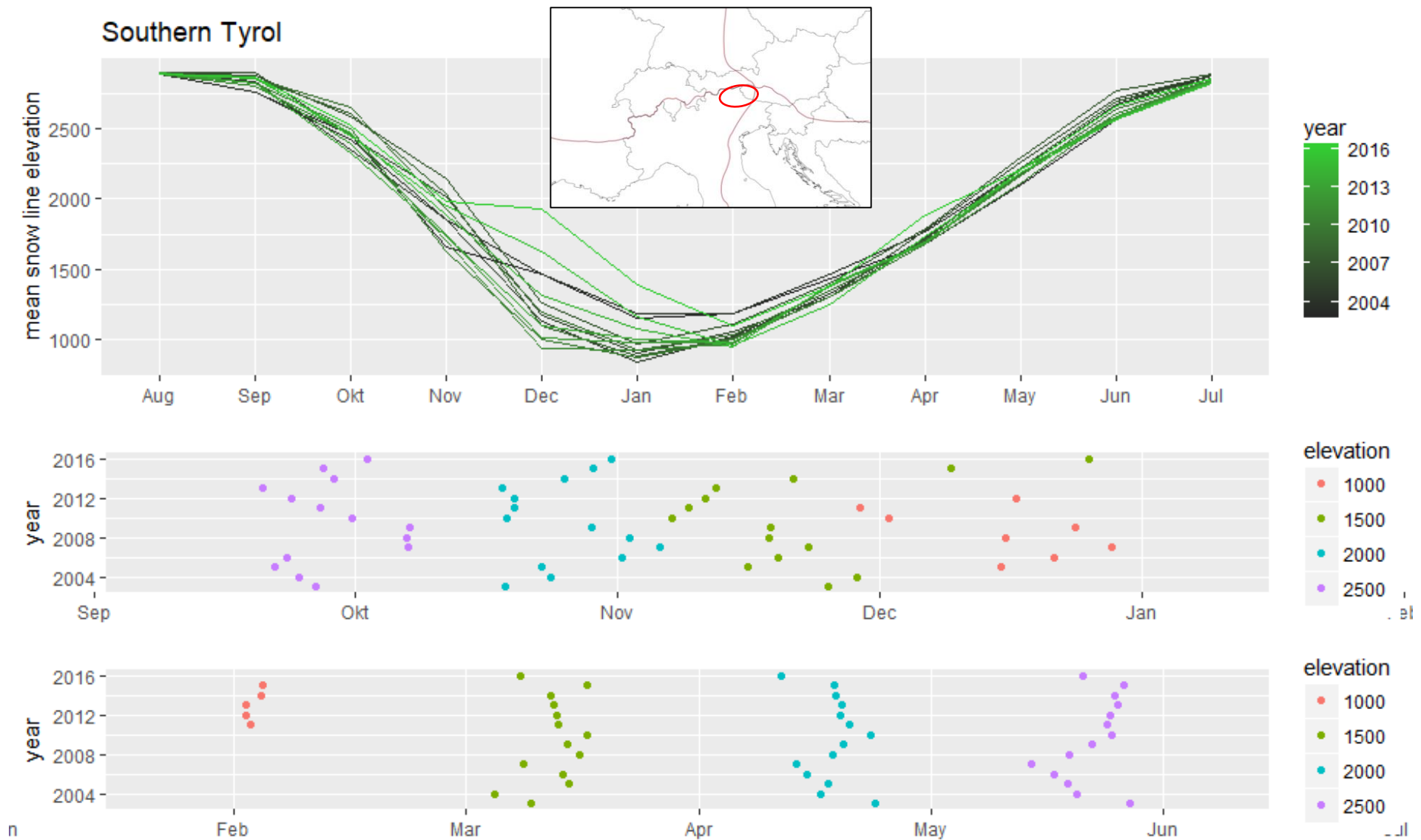


Fig. R3 upper panel: Average snowline elevations for tiles in Southern Tyrol; monthly means per year; rolling mean with a width of 4 years was applied; middle and lower panel: dates of snowline 'crossing' selected elevations for autumn (middle) and spring (lower);

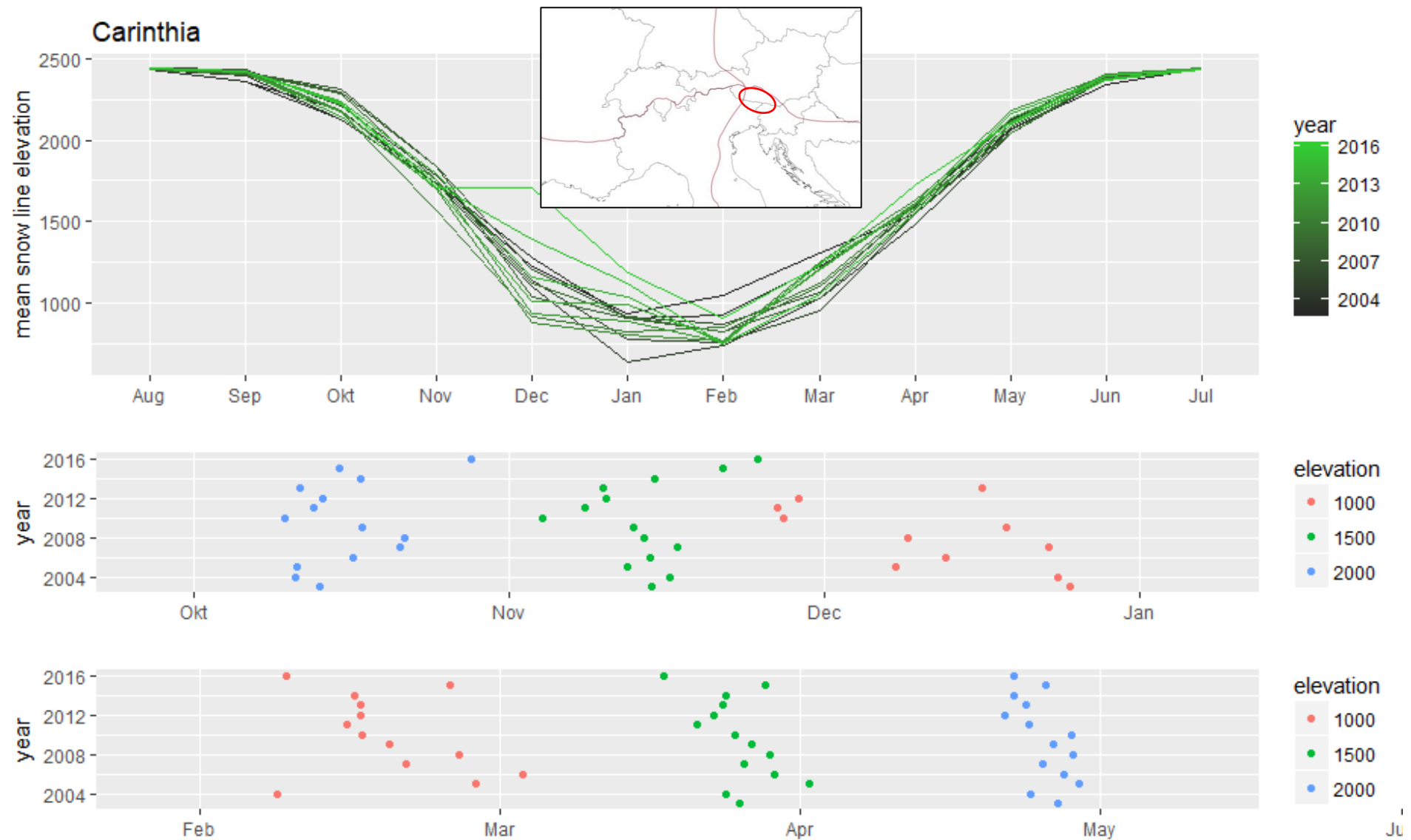


Fig. R4 upper panel: Average snowline elevations for tiles in Carinthia; monthly means per year; rolling mean with a width of 4 years was applied; middle and lower panel: dates of snowline 'crossing' selected elevations for autumn (middle) and spring (lower);

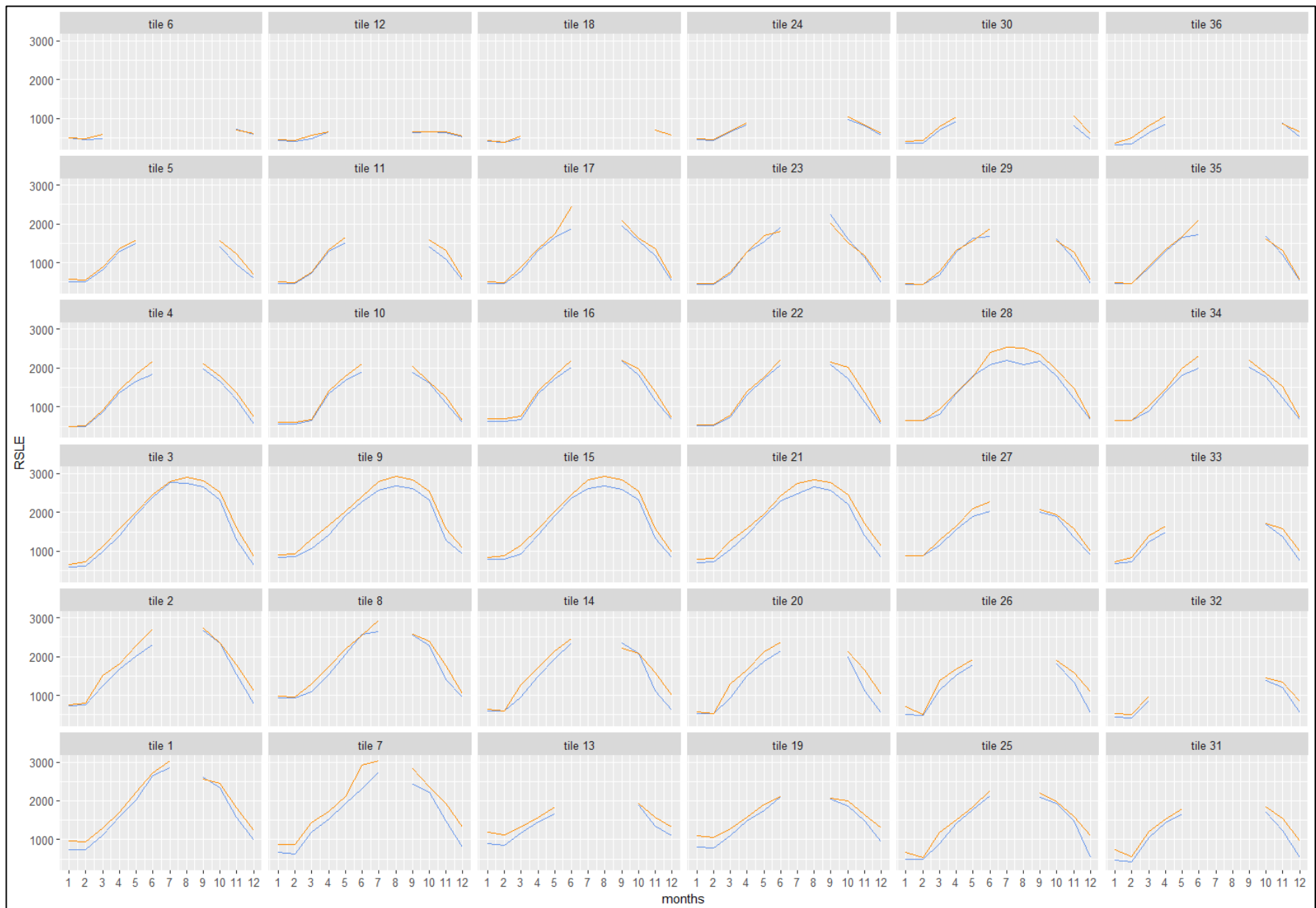


Fig. R5: Comparison of long-term monthly mean snowline elevations in two exposition classes: high solar radiation sum (orange) and low solar radiation sum (blue);

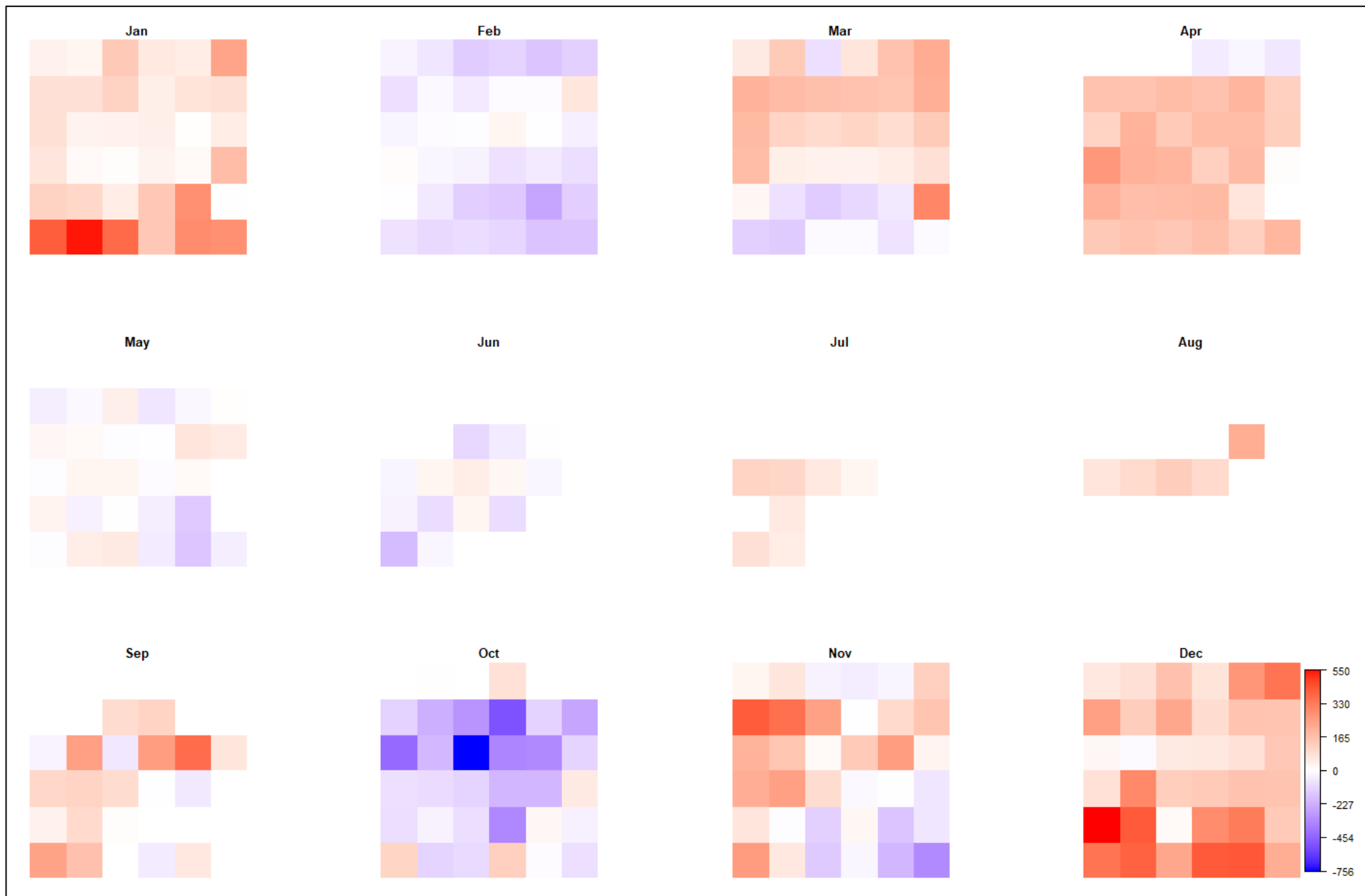


Fig. R6: low solar radiation sum; changes in snowline elevation based on linear trend for the period 2000-2017;



Fig. R7: low solar radiation sum; changes in snowline elevation;
 based on linear trend for the period 2000-2017;

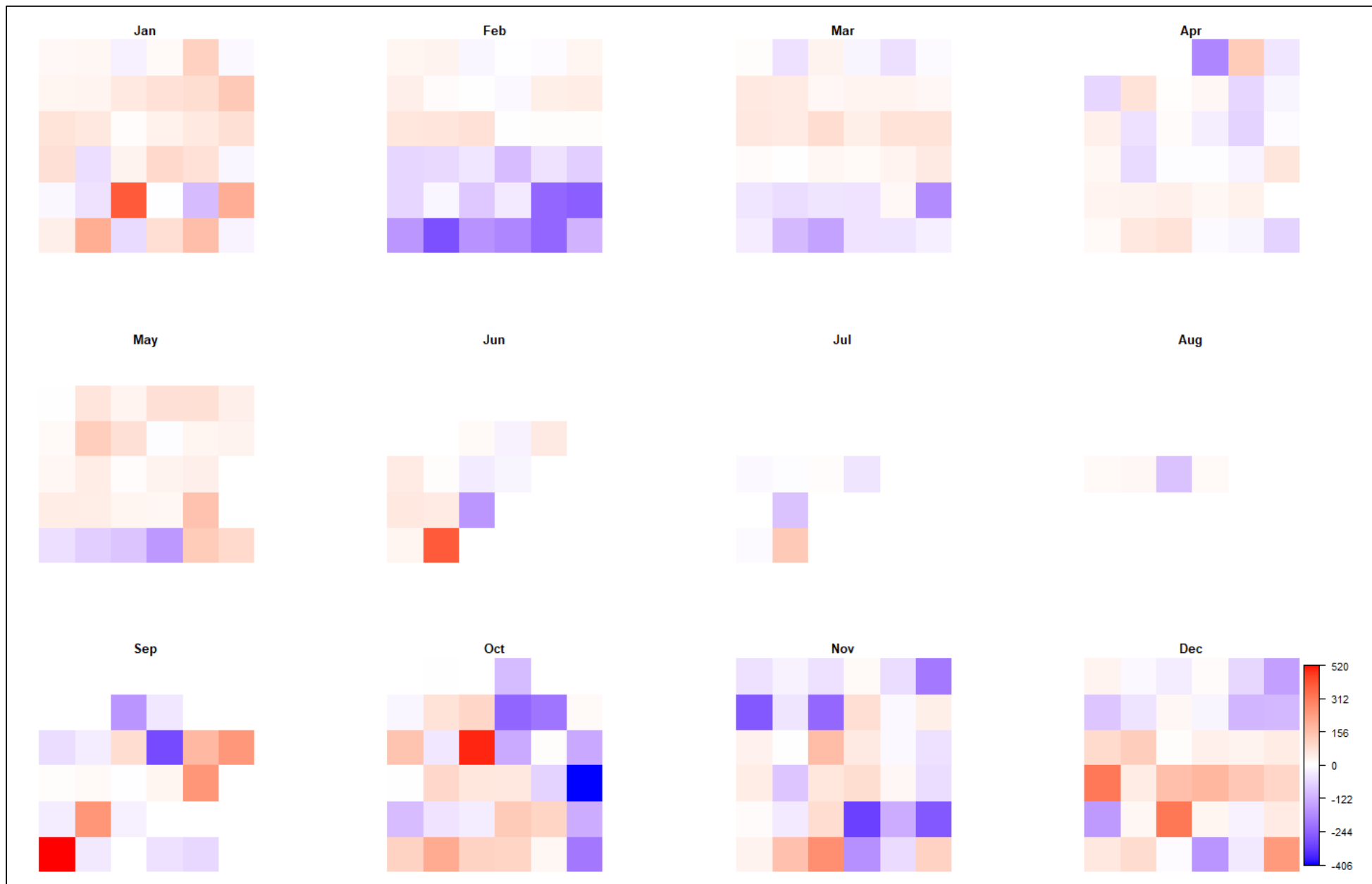


Fig. R8: Changes in the difference between snowlines at low and high solar radiation sum; based on linear trend for 2000-2017;

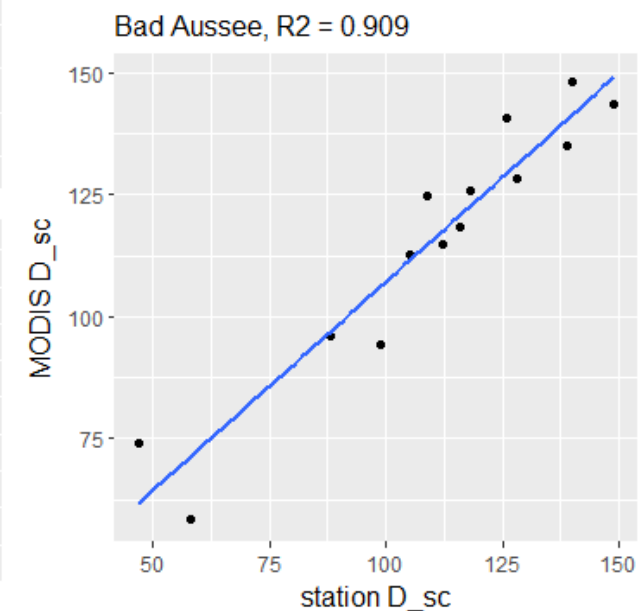
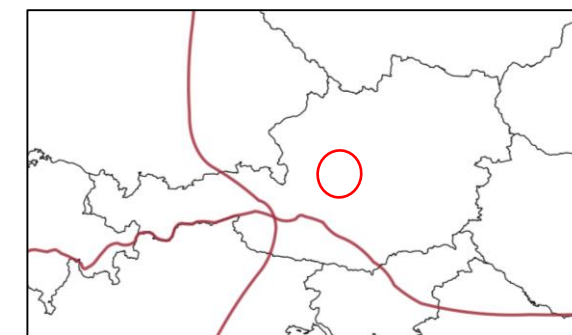
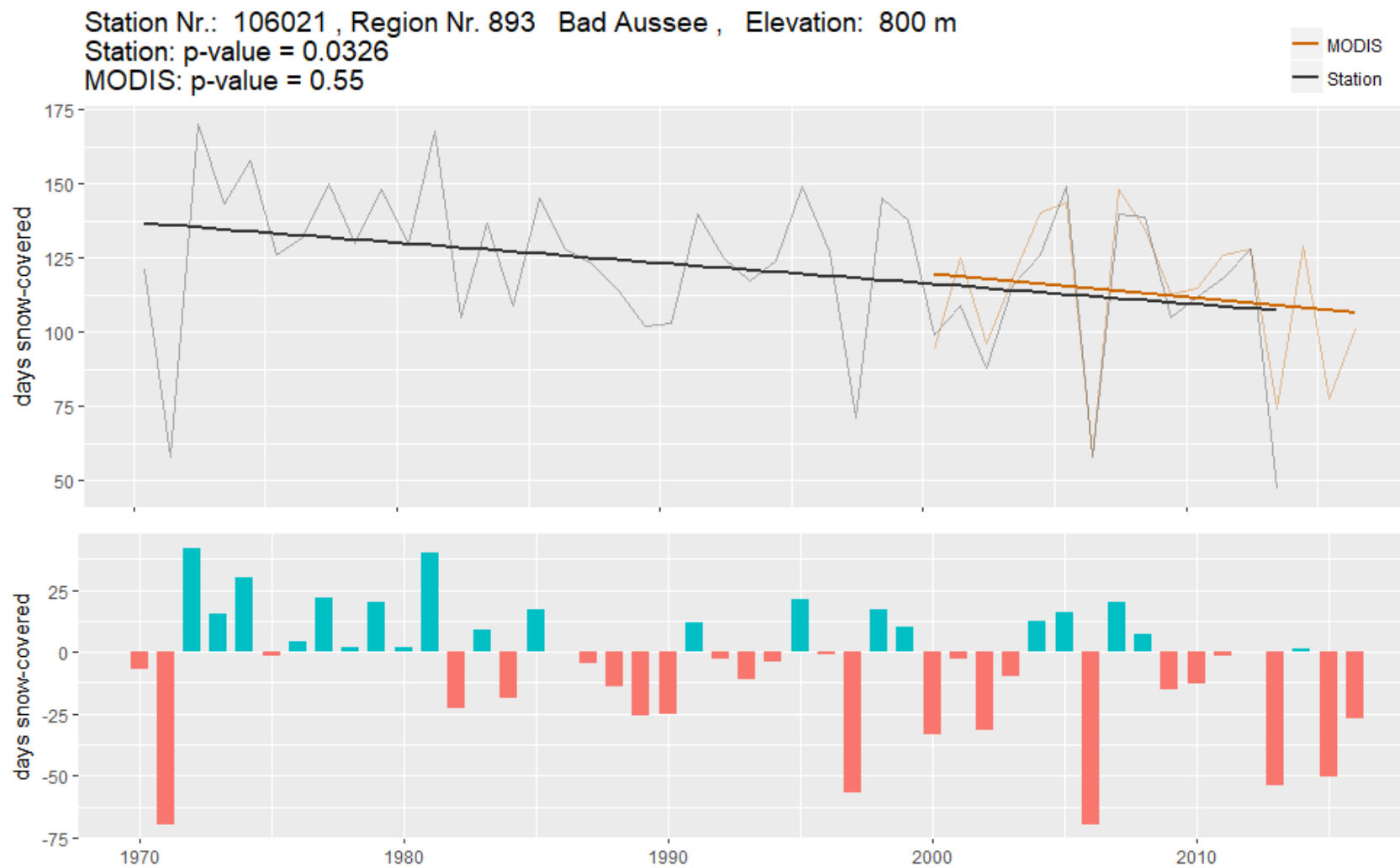


Fig. R9, upper left: comparison of MODIS derived D_{sc} and long-term station D_{sc} for Bad Aussee; lower left: Anomalies of yearly D_{sc} ; reference: mean of long term station values; plot shows station data until 2000 and MODIS results onwards; lower right: Correlation of station vs. MODIS D_{sc} for the common period (2000-2014);

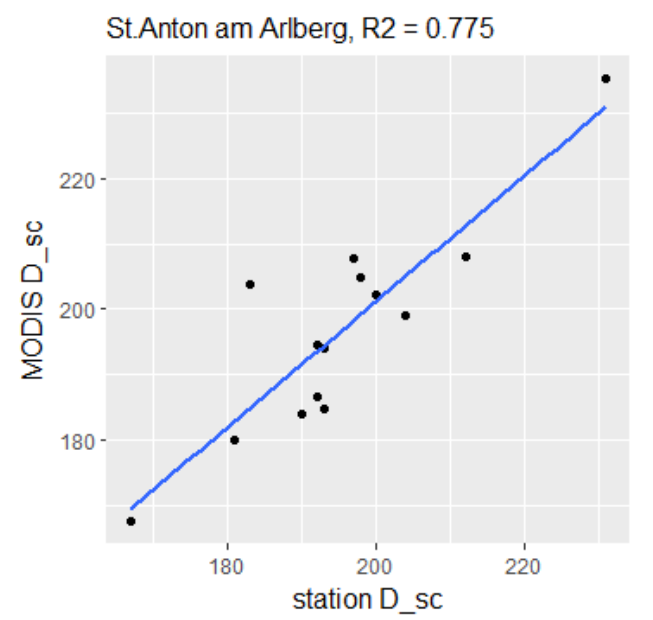
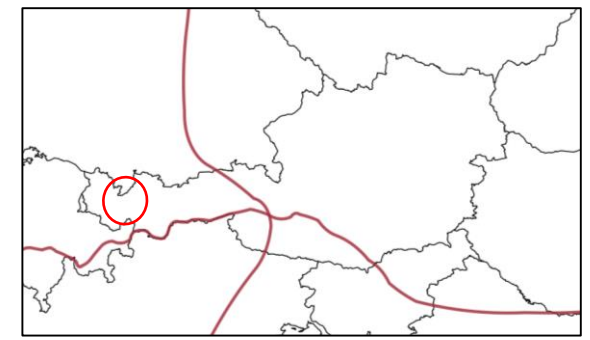
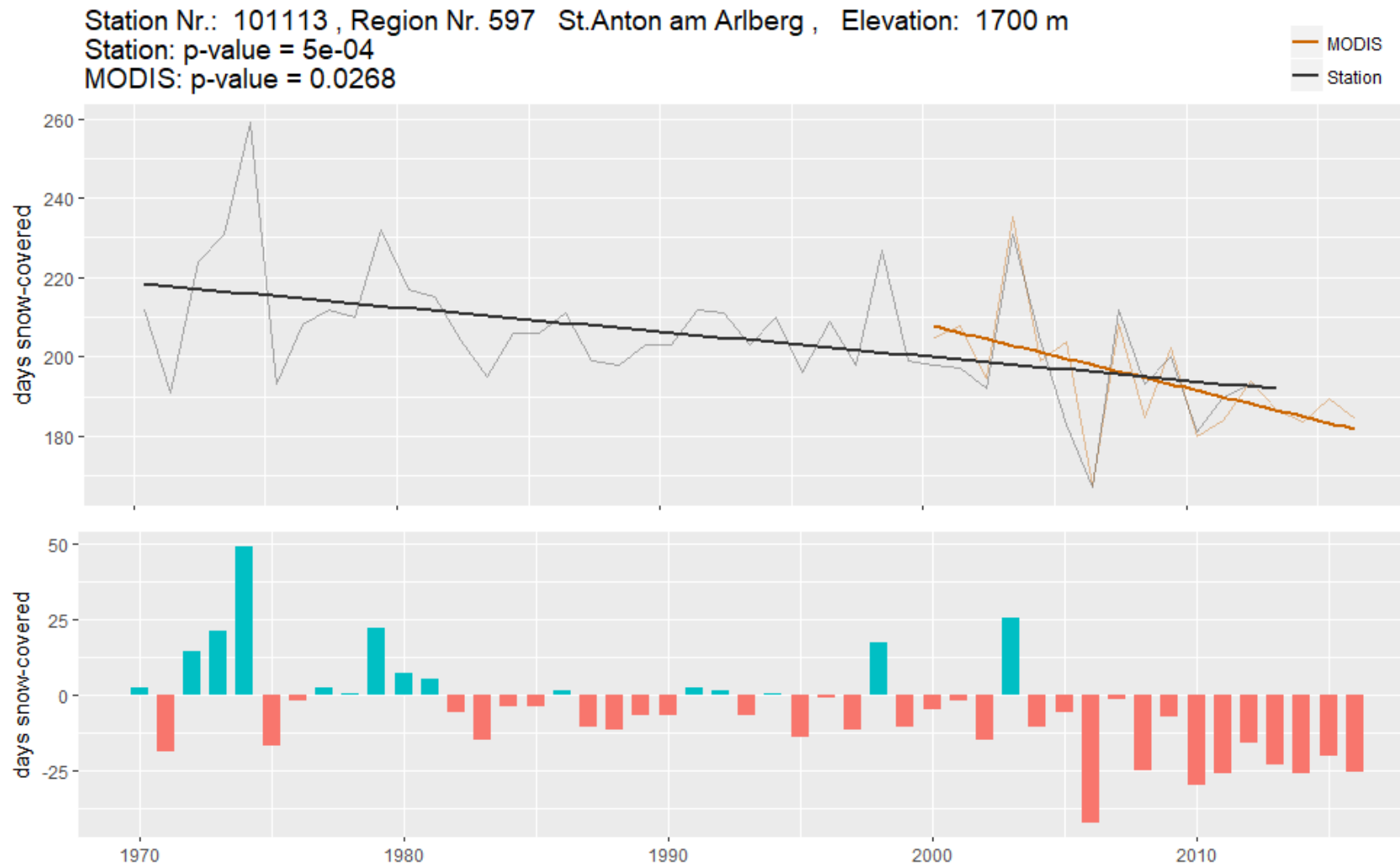


Fig. R10, upper left: comparison of MODIS derived D_{sc} and long-term station D_{sc} for St.Anton am Arlberg; lower left: Anomalies of yearly D_{sc} ; reference: mean of long term station values; plot shows station data until 2000 and MODIS results onwards; lower right: Correlation of station vs. MODIS D_{sc} for common period (2000-2014);

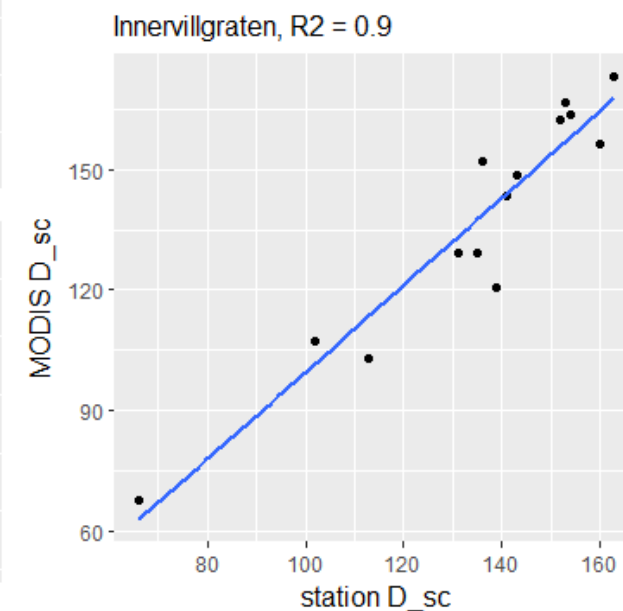
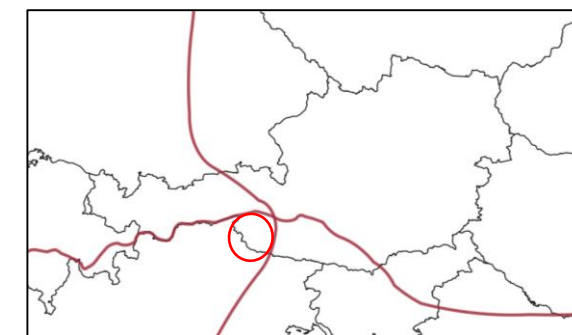
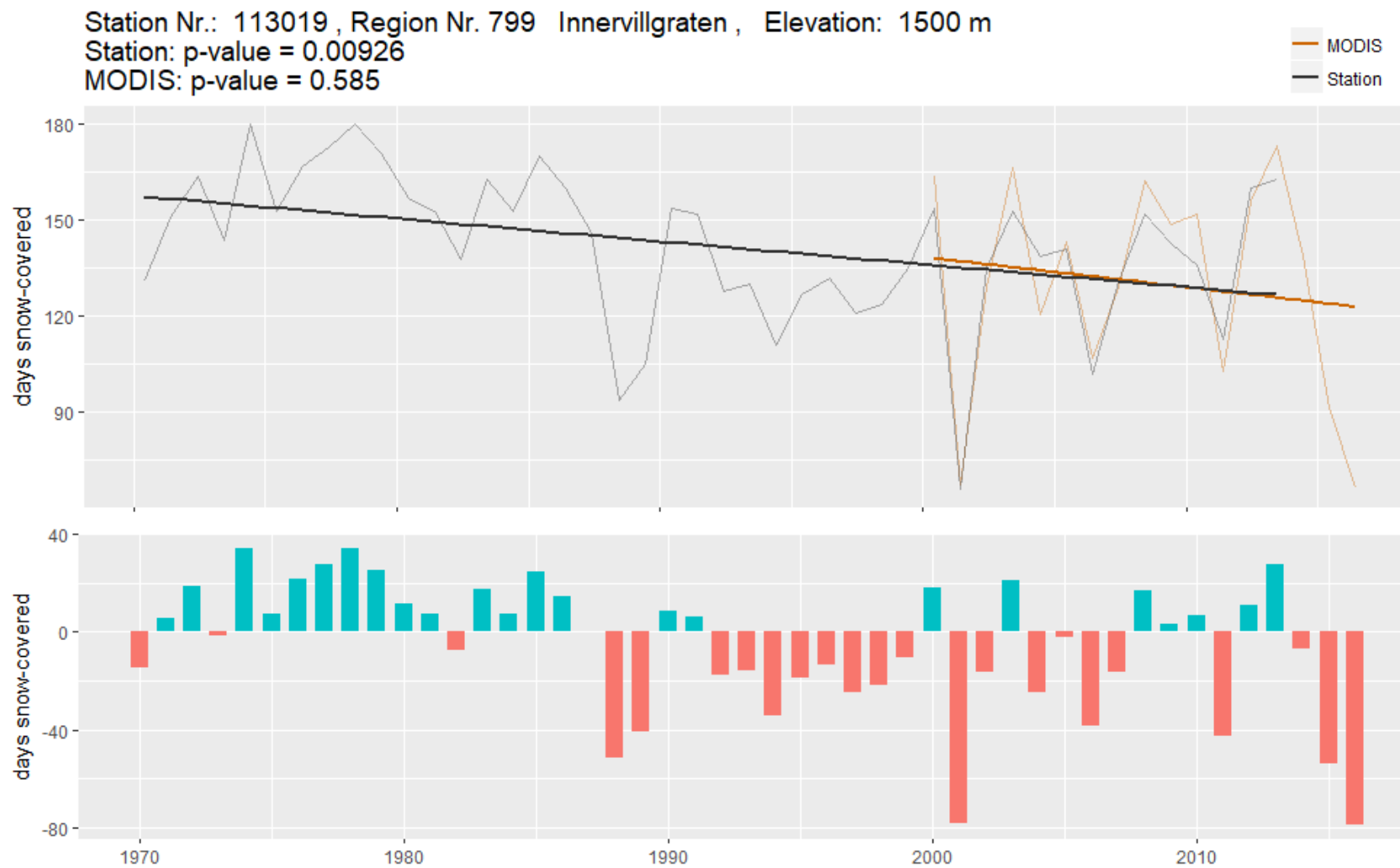


Fig. R11, upper left: comparison of MODIS derived D_{sc} and long-term station D_{sc} for Innervillgraten; lower left: Anomalies of yearly D_{sc} ; reference: mean of long term station values; plot shows station data until 2000 and MODIS results onwards; lower right: Correlation of station vs. MODIS D_{sc} for common period (2000-2014);

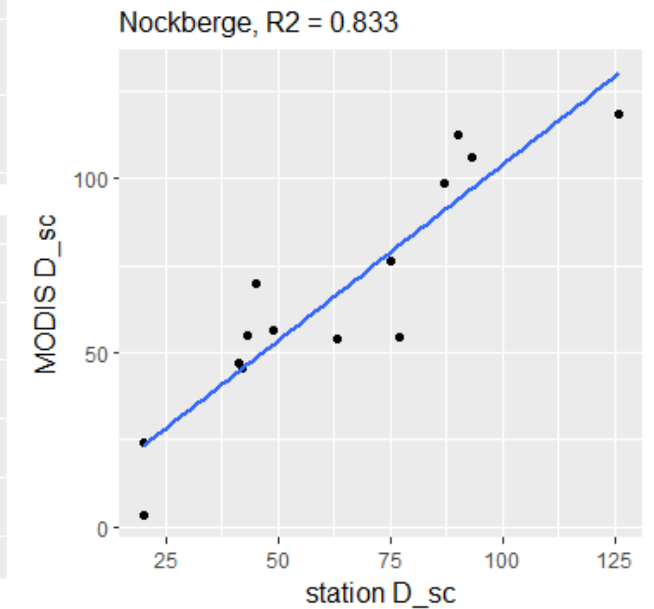
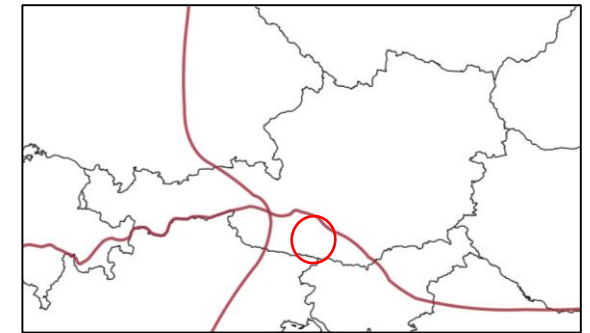
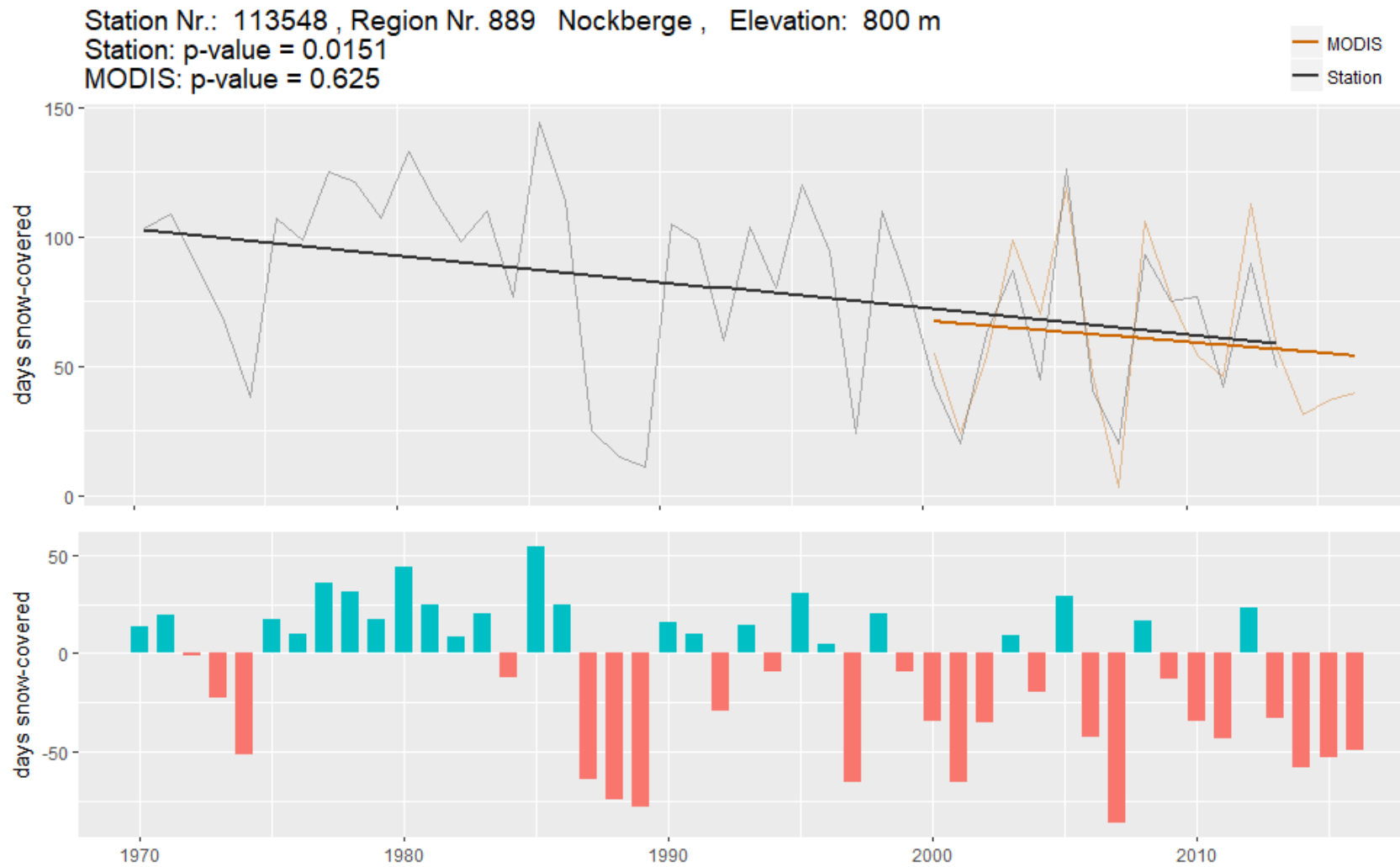


Fig. R12, upper left: comparison of MODIS derived D_{sc} and long-term station D_{sc} for Nockberge; lower left: Anomalies of yearly D_{sc} ; reference: mean of long term station values; plot shows station data until 2000 and MODIS results onwards; lower right: Correlation of station vs. MODIS D_{sc} for common period (2000-2014);

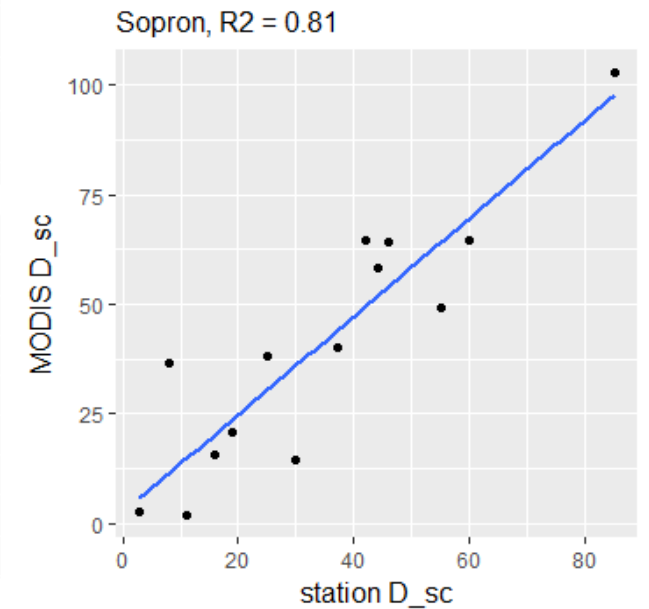
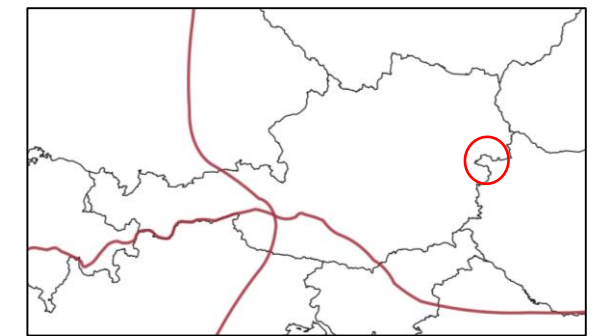
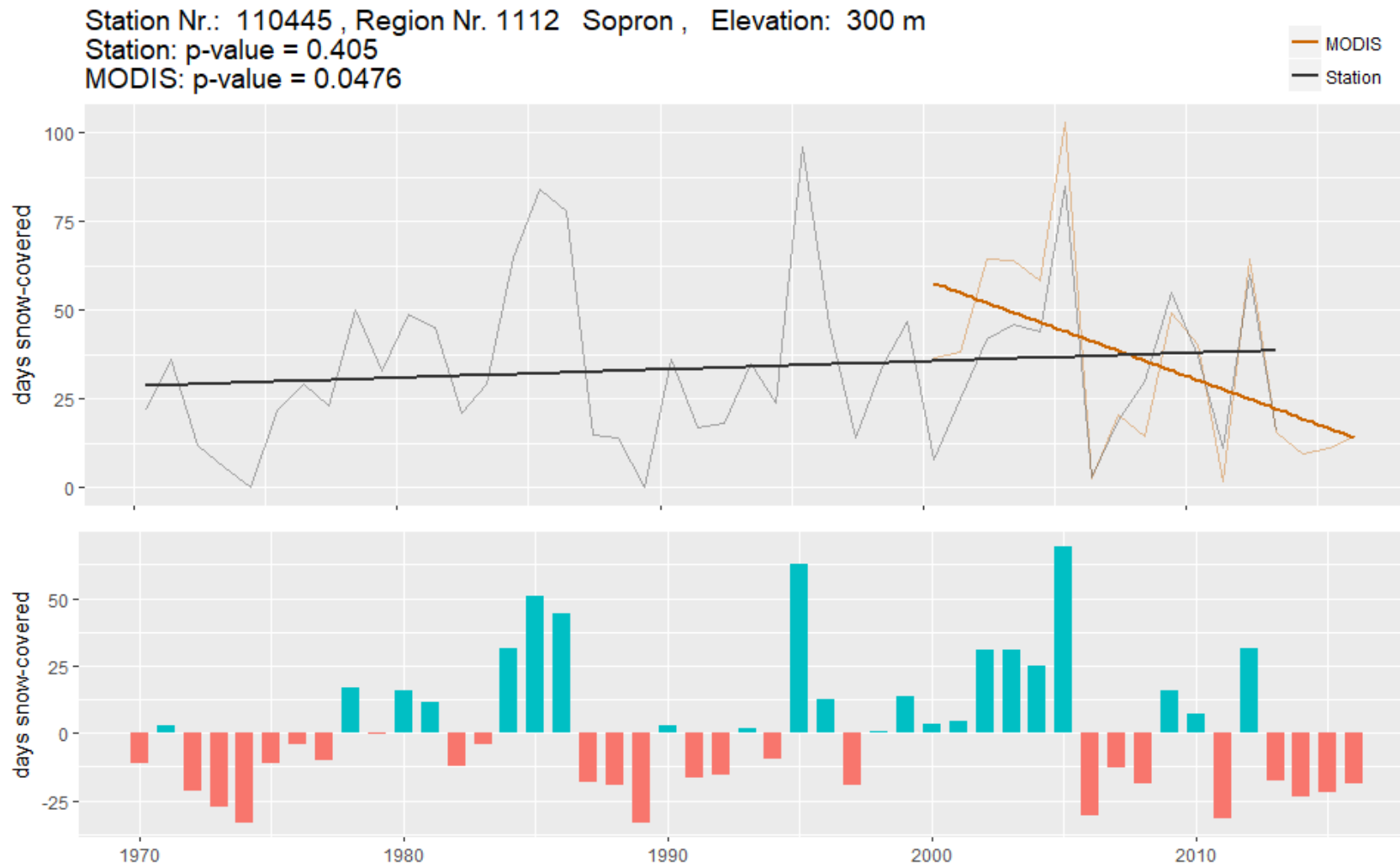


Fig. R13, upper left: comparison of MODIS derived D_{sc} and long-term station D_{sc} for Sopron; lower left: Anomalies of yearly D_{sc} ; reference: mean of long term station values; plot shows station data until 2000 and MODIS results onwards; lower right: Correlation of station vs. MODIS D_{sc} for common period (2000-2014);

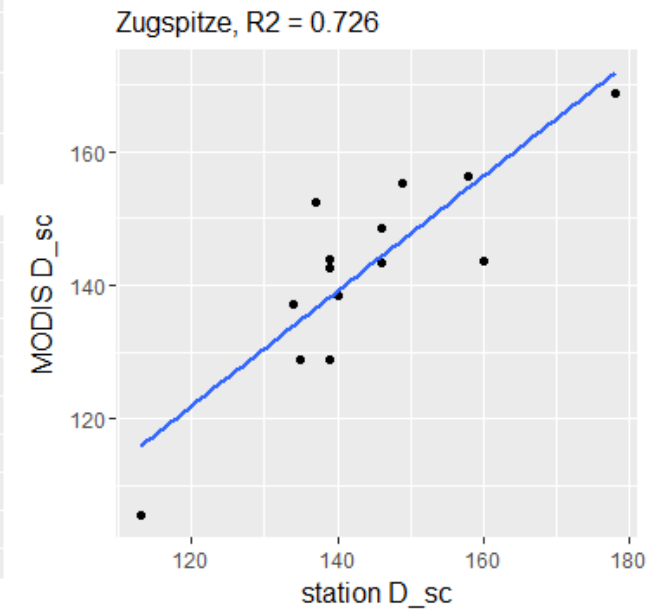
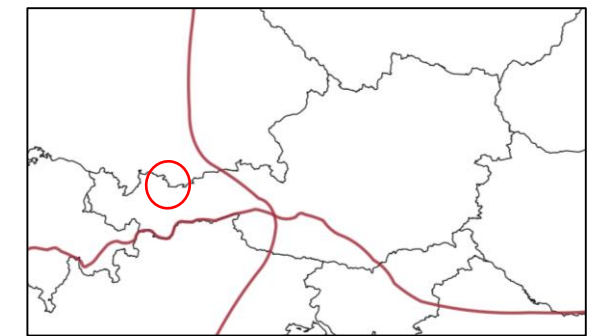
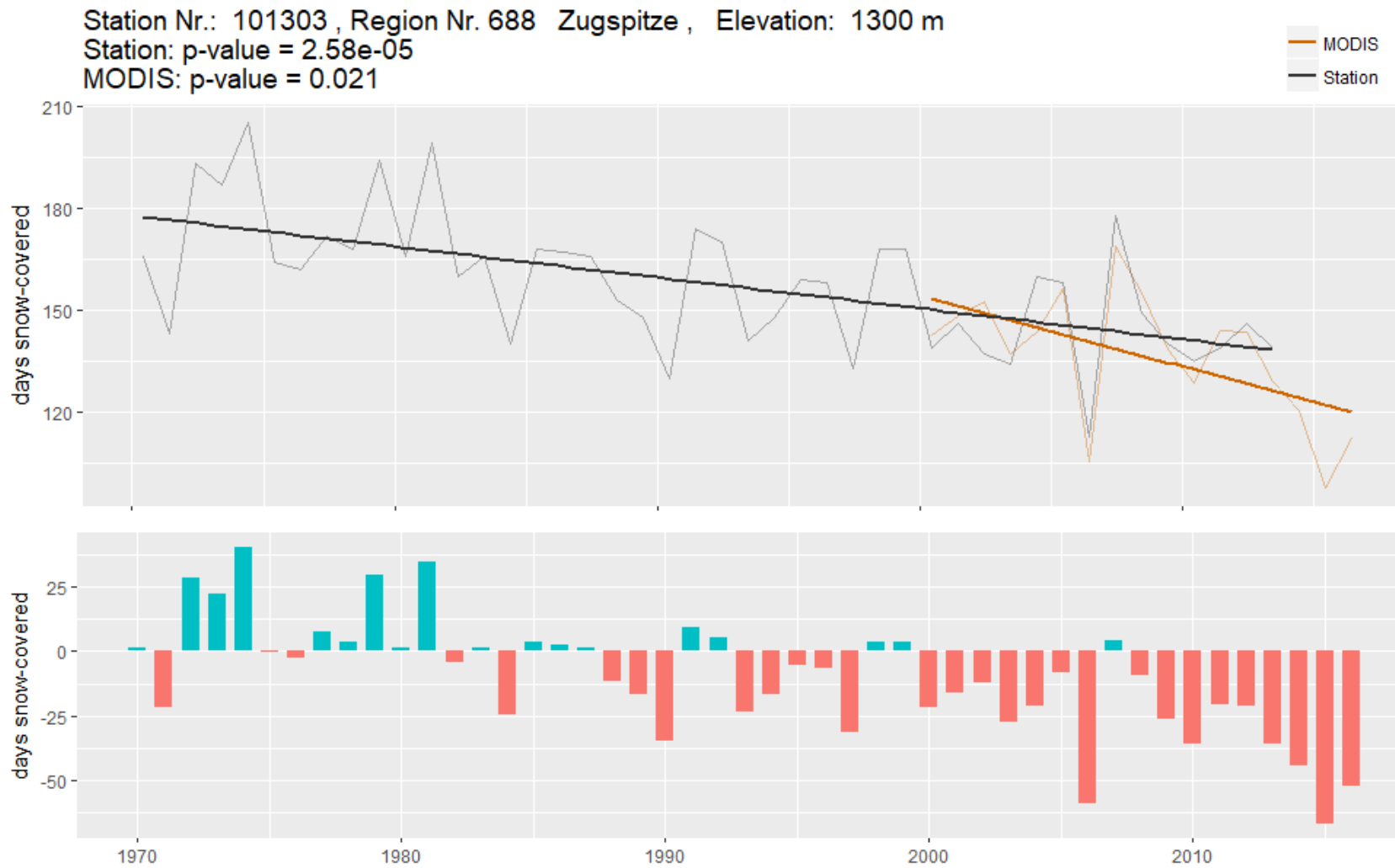


Fig. R14, upper left: comparison of MODIS derived D_{sc} and long-term station D_{sc} for Zugspitze; lower left: Anomalies of yearly D_{sc} ; reference: mean of long term station values; plot shows station data until 2000 and MODIS results onwards; lower right: Correlation of station vs. MODIS D_{sc} for common period (2000-2014);

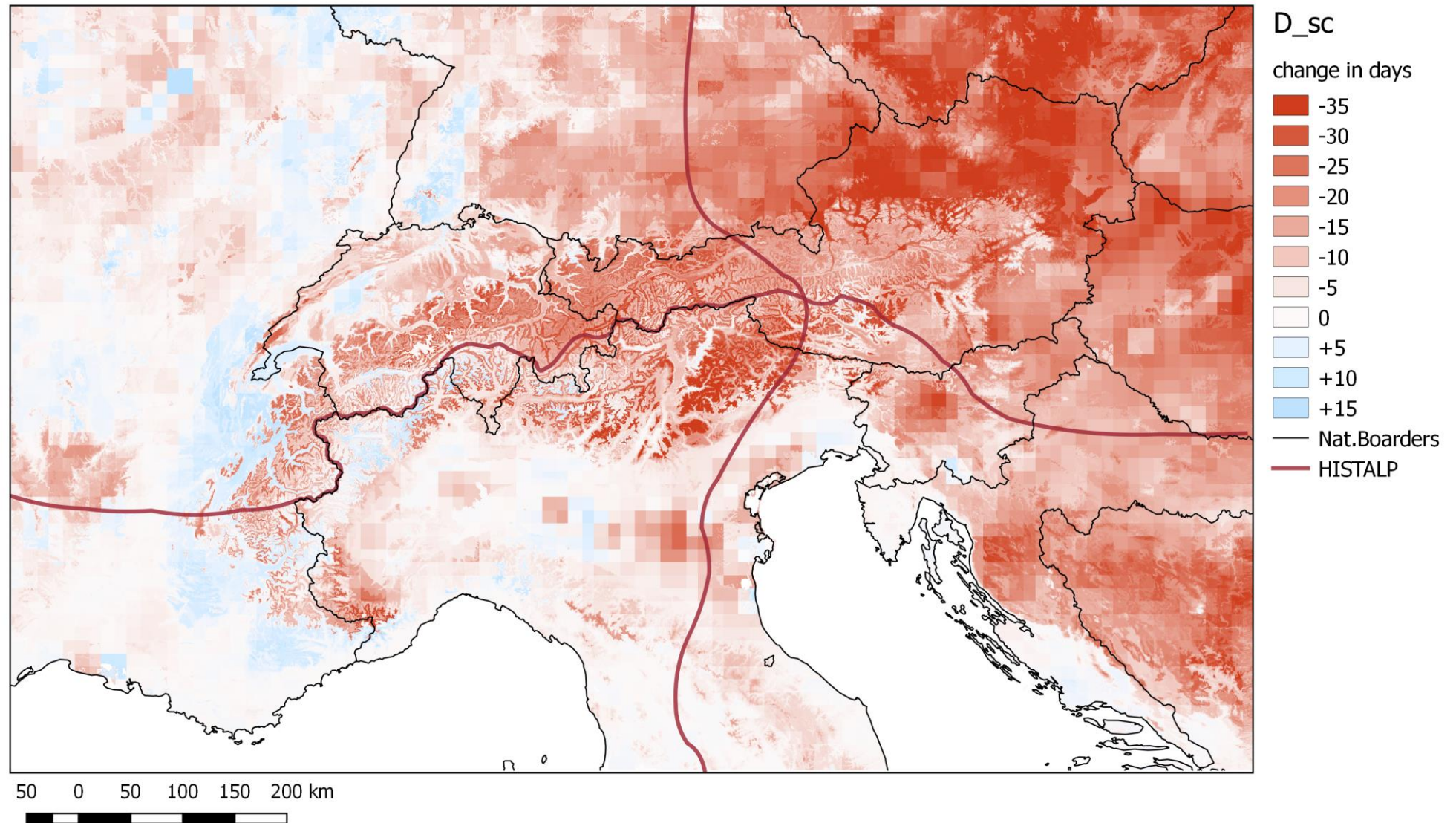


Fig. R15: Change in annual snow covered days (D_{sc}) according to linear trend analysis; Days with snow cover (above RSLE) were calculated for seasons (Aug. 16 – Aug. 15); linear trend was applied for the period 2000-2017, for each of the 2500 overlapping regions; Map contains significant and non-significant trends;

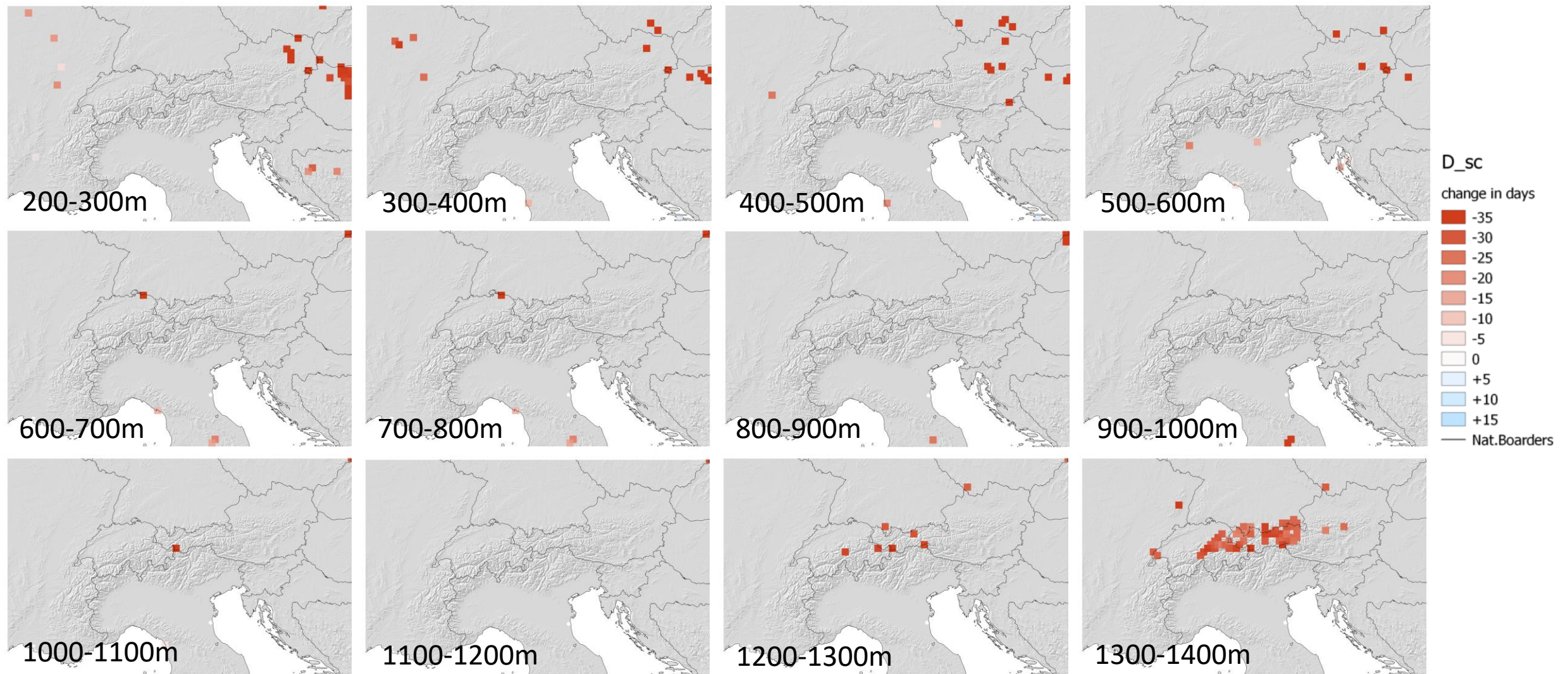


Fig. R16: Change in annual snow covered days (D_{sc}) according to linear trend analysis in 100m elevation steps; Days with snow cover (above RSLE) were calculated for seasons (August – August); linear trend was applied for period 2000-2017; Maps show significant trends only (p -value $\leq 0,05$); Elevations in m.a.s.l.;

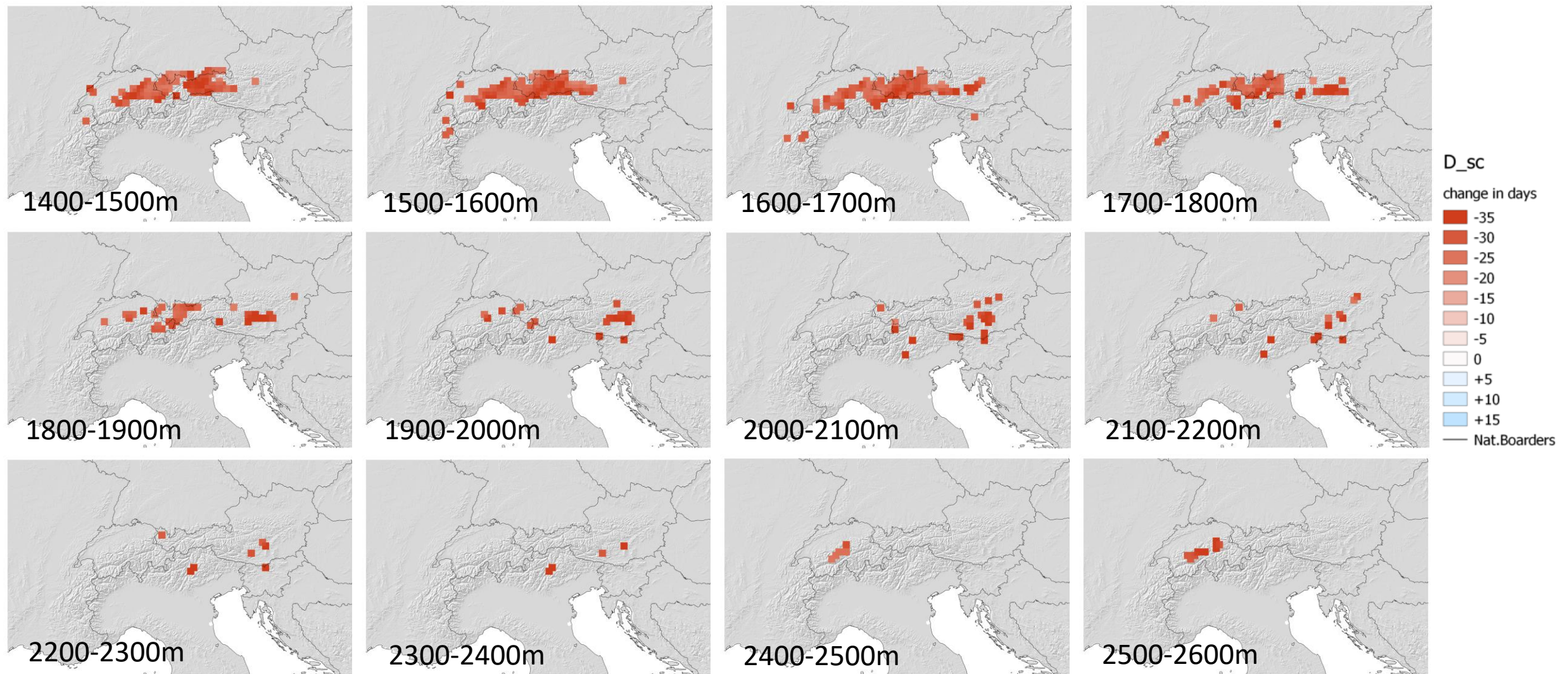


Fig. R17: Change in annual snow covered days (D_{sc}) according to linear trend analysis in 100m elevation steps; Days with snow cover (above RSLE) were calculated for seasons (August – August); linear trend was applied for period 2000-2017; Maps show significant trends only (p -value $\leq 0,05$); Elevations in m.a.s.l.;

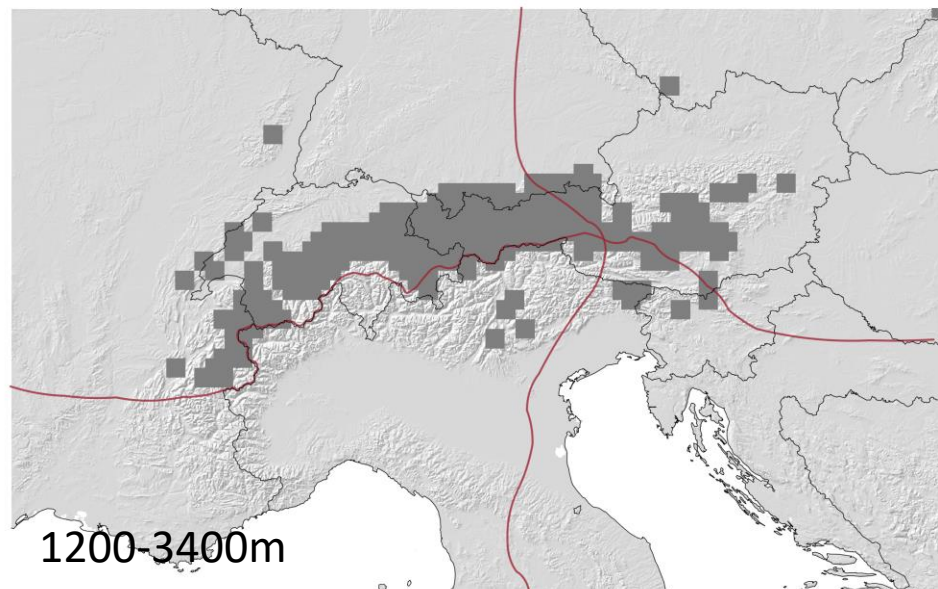
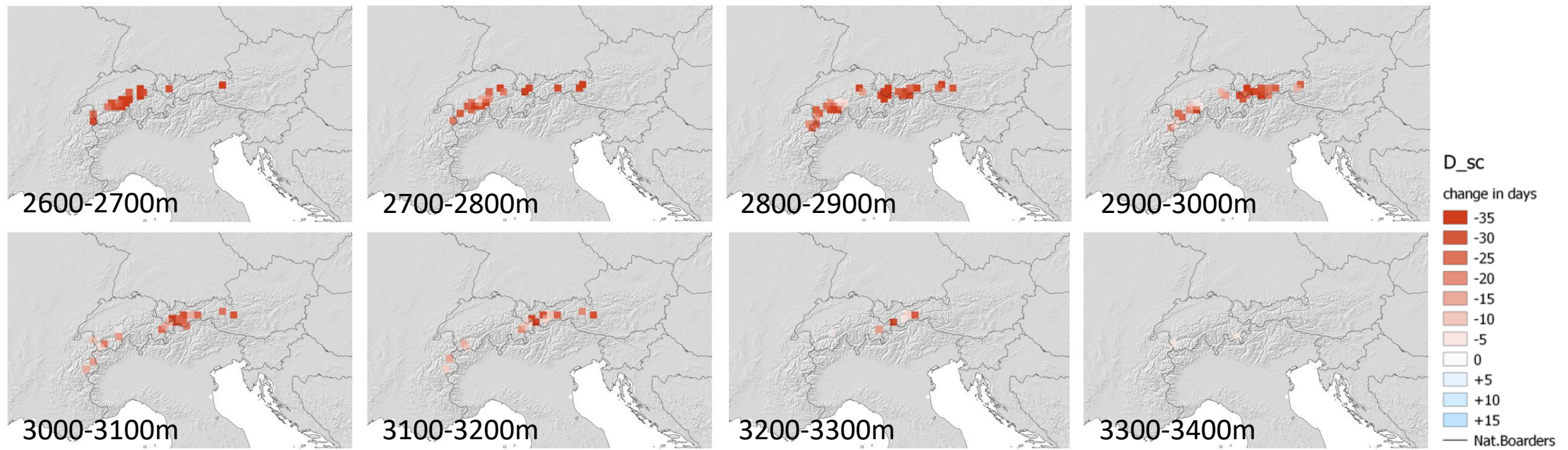


Fig. R18, first 8 panels: Change in annual snow covered days (D_{sc}) according to linear trend analysis in 100m elevation steps; Days with snow cover (above RSLE) were calculated for seasons (August – August); linear trend was applied for period 2000-2017; Maps show significant trends only (p -value $\leq 0,05$);

last panel: spatial distribution of significant trends between 1200 and 3400 m.a.s.l. (dark grey fields) and horizontal climatic sub-regions of the GAR (red lines); Elevations in m.a.s.l.;

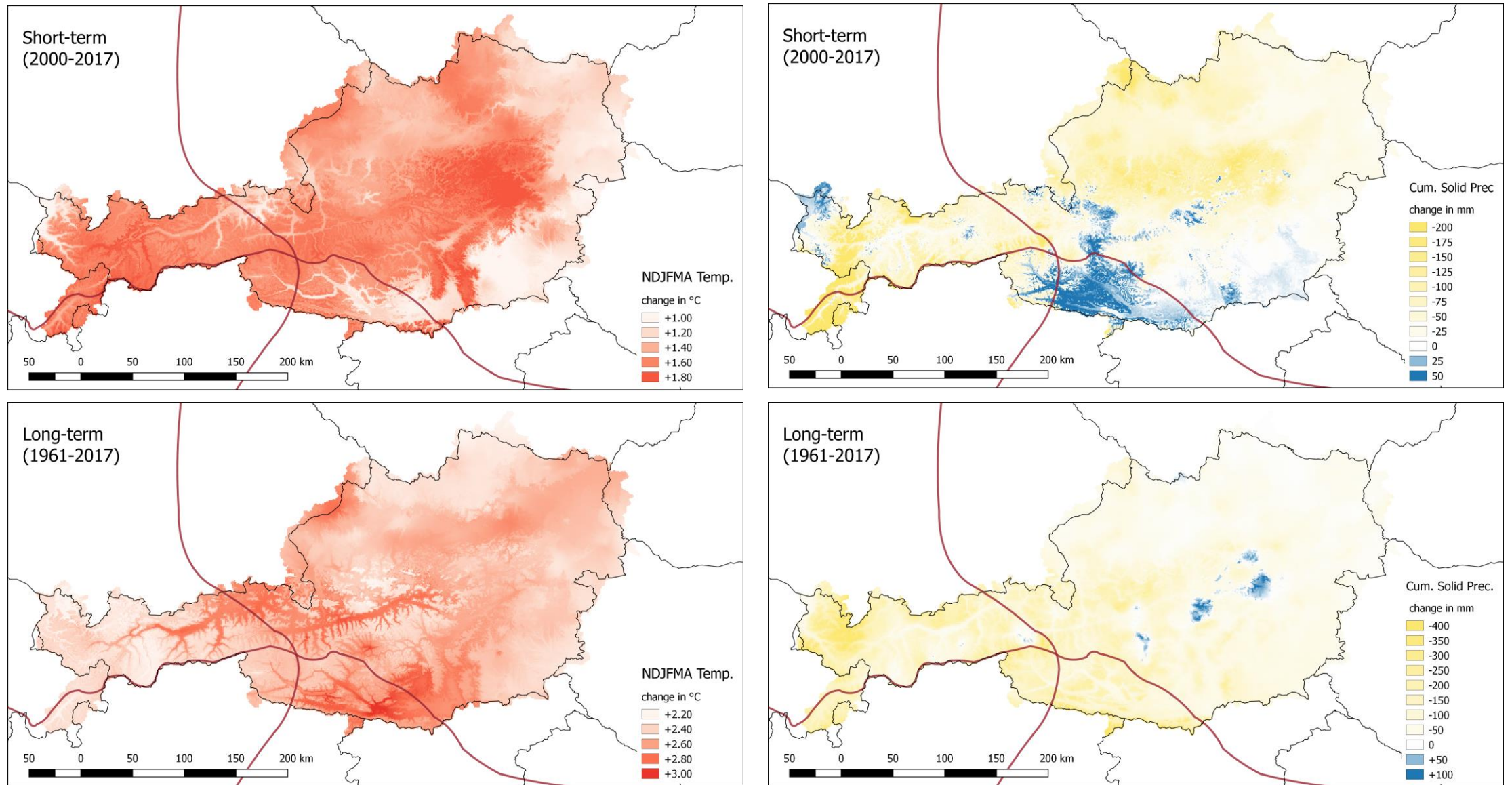


Fig. R19: Short- and long-term trends of winter (NDJFMA) temperature and cumulative solid precipitation for Austria; linear trend, significant and non-significant values;

Northern Austria

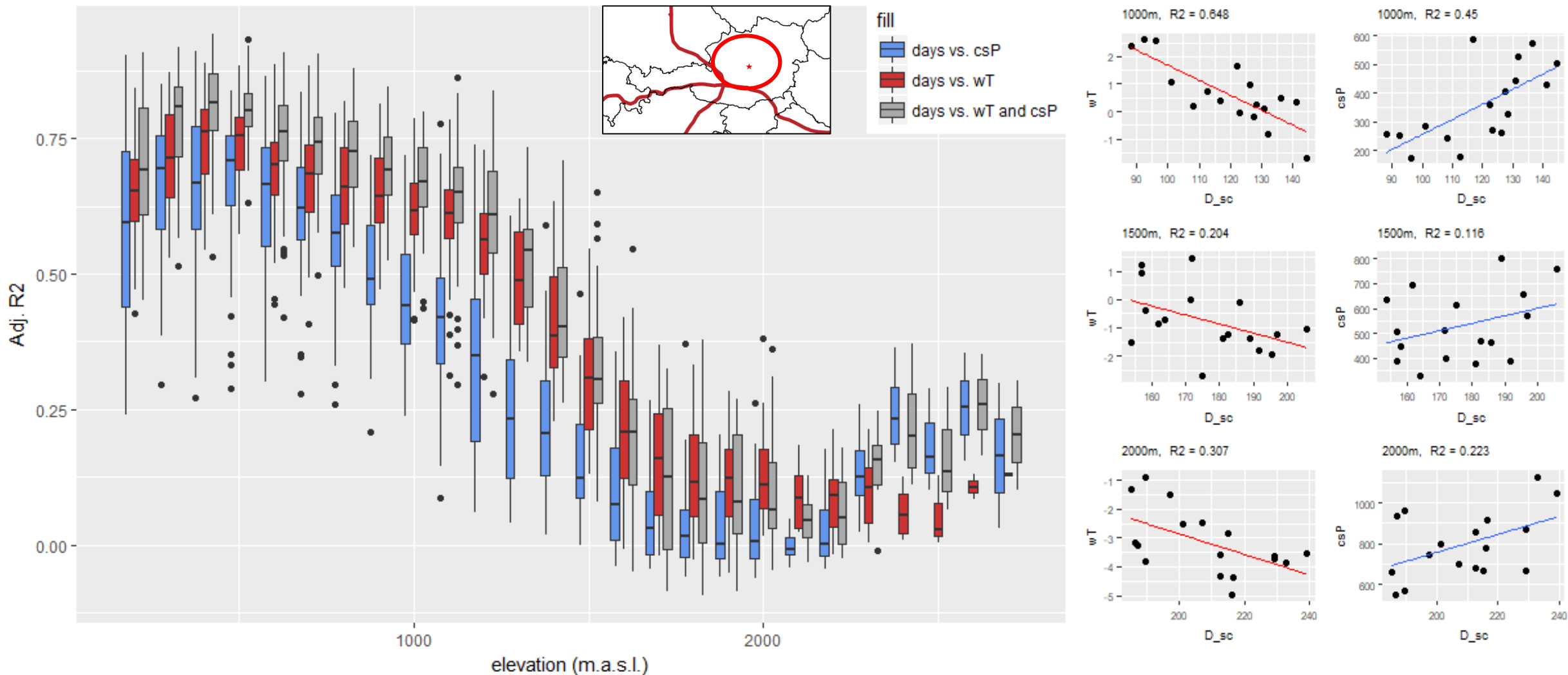


Fig. R20, left: Boxplots of Adjusted R^2 from simple regression (D_{sc} vs. Precipitation, D_{sc} vs. Temperature) and multiple regression (D_{sc} vs Precipitation + Temperature) for Northern Austria; right: correlations of D_{sc} to temperature and precipitation for selected elevations; one tile was used for correlations as indicated with red star in map;

Southern Austria

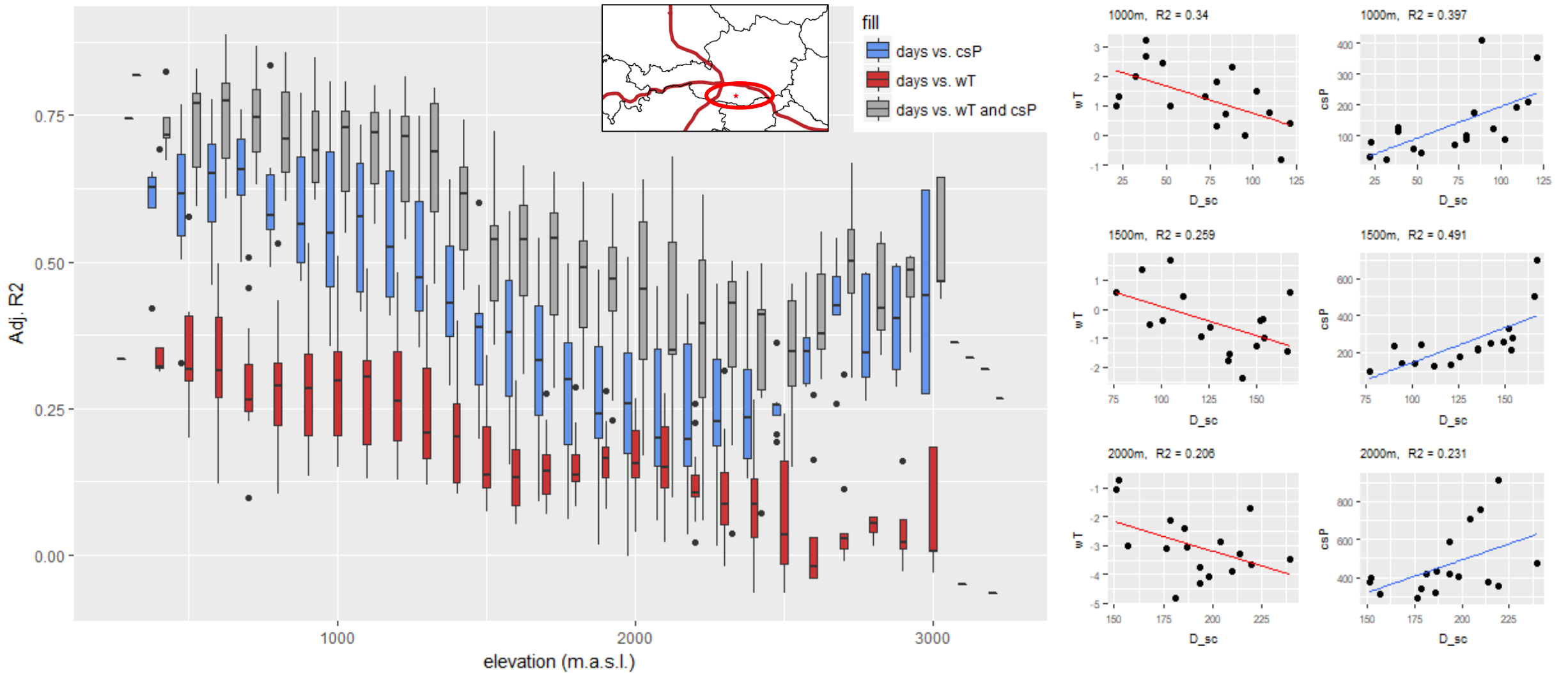


Fig. R21, left: Boxplots of Adjusted R^2 from simple regression (D_{sc} vs. Precipitation, D_{sc} vs. Temperature) and multiple regression (D_{sc} vs Precipitation + Temperature) for Southern Austria; right: correlations of D_{sc} to wT and csP for selected elevations; one tile was used for correlations as indicated with red star in map;

Vorarlberg/Tirol

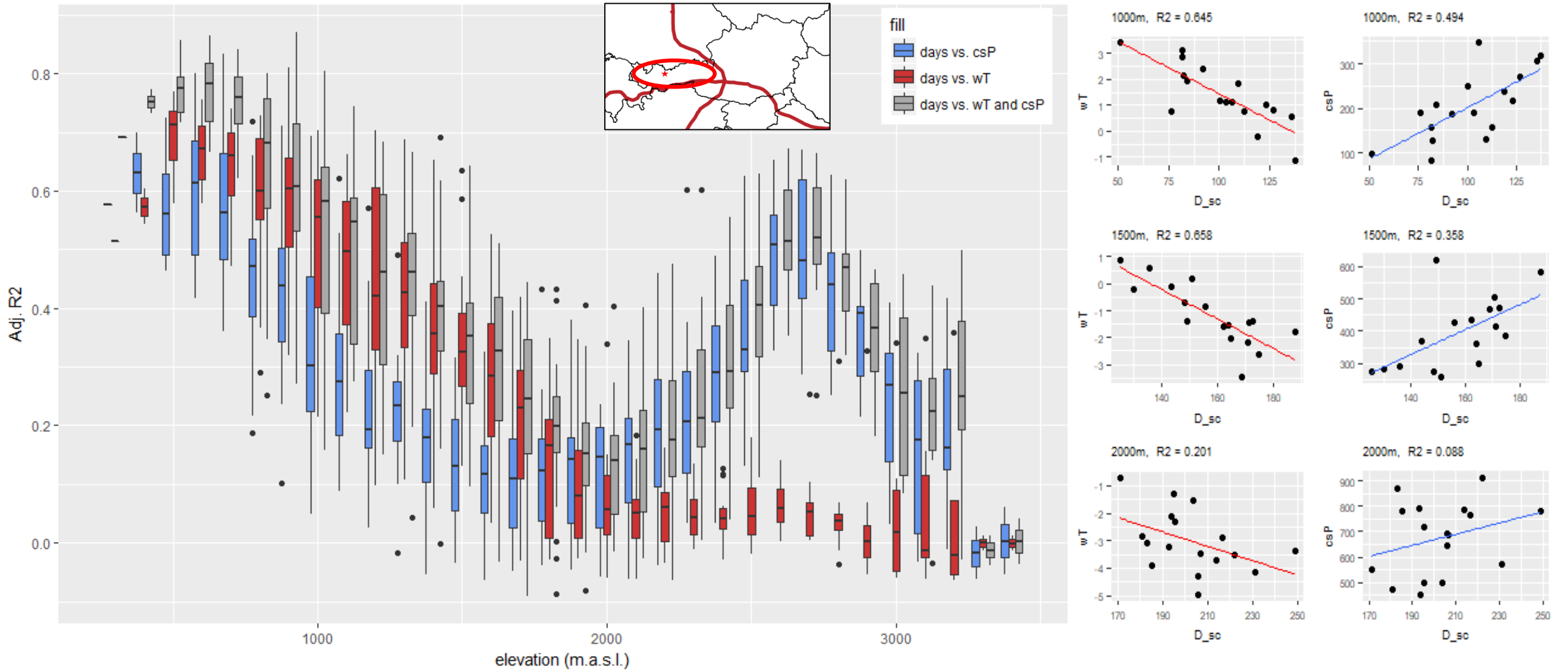


Fig. R22, left: Boxplots of Adjusted R² from simple regression (D_{sc} vs. Precipitation, D_{sc} vs. Temperature) and multiple regression (D_{sc} vs Precipitation + Temperature) for Vorarlberg/Tirol; right: correlations of D_{sc} to wT and csP for selected elevations; one tile was used for correlations as indicated with red star in map;